BRNO UNIVERSITY OF TECHNOLOGY
VYSOKÉ UČENÍ TECHNICKÉ V BRNĚ

FACULTY OF ELECTRICAL ENGINEERING AND COMMUNICATION
FAKULTA ELEKTROTECHNIKY
A KOMUNIKAČNÍCH TECHNOLOGIÍ

DEPARTMENT OF BIOMEDICAL ENGINEERING
ÚSTAV BIOMEDICÍNSKÉHO INŽENÝRSTVÍ

THE CELL MIGRATION MONITORING IN A MICROFLUIDIC SYSTEM BY THE "SCRATCH WOUND HEALING ASSAY" METHOD
SLEDOVÁNÍ MIGRACE BUNĚK V MIKROFLUIDNÍM SYSTÉMU METODOU „SCRATCH WOUND HEALING ASSAY"

MASTER'S THESIS
DIPLOMOVÁ PRÁCE

AUTHOR   Bc. Katsiarina Morgaenko
AUTOR PRÁCE

SUPERVISOR   Larisa Baiazitova
VEDOUCÍ PRÁCE

BRNO 2019

Diplomová práce

magisterský navazující studijní obor **Biomedicínské a ekologické inženýrství**

Ústav biomedicínského inženýrství

Studentka: Bc. Katsiarina Morgaenko   *ID:* 164213

Ročník: 2   *Akademický rok:* 2018/19

NÁZEV TÉMATU:

Sledování migrace buněk v mikrofluidním systému metodou „Scratch Wound Healing Assay"

POKYNY PRO VYPRACOVÁNÍ:

1) Nastudujte kultivaci buněčné linie 3T3 a HUVEC. 2) Proveďte literární rešerši v oblasti kultivace buněk v mikrofluidních systémech simulujících kapiláry a aplikace experimentu "Scratch Wound Healing Assay" v těchto podmínkách. 3) Navrhněte experiment s použitím fluorescenčního nebo konfokálního mikroskopu. 4) Kultivaci buněk ověřte v buněčné laboratoři. 5) Navržený experiment otestujte s dostatečným počtem opakování. 6) Proveďte sběr mikroskopických dat. Ve vhodném programovém prostředí zpracujte nasnímaná data. 7) Dosažené výsledky vhodně prezentujte a proveďte diskuzi.

DOPORUČENÁ LITERATURA:

[1] VAN DER MEER, Andries D., et al. A microfluidic wound-healing assay for quantifying endothelial cell migration. American Journal of Physiology-Heart and Circulatory Physiology, 2010, 298.2: H719-H725.

[2] NIE, Fu-Qiang, et al. On-chip cell migration assay using microfluidic channels. Biomaterials, 2007, 28.27: 4017-4022.

Termín zadání: 4.2.2019   *Termín odevzdání:* 17.5.2019

Vedoucí práce: Larisa Baiazitova
Konzultant:

prof. Ing. Ivo Provazník, Ph.D.
předseda oborové rady

ABSTRAKT

Tato diplomová práce se zabývá popisem principů kultivace embryonálních fibroblastových buněk myší (3T3), lidských endoteliálních buněk odebraných z pupečníkové žíly (HUVEC) a epiteliálních buněk vaječníku čínského křečka (CHO) v mikrofluidních systémech simulujících kapiláry. Byly provedeny literární rešerše v oblasti realizací experimentu *"Scratch Wound Healing Assay"* v mikrofluidních systémech s použitím fibroblastů a endotheliálních buněk. V práci jsou dále popsány principy konfokální a fluorescenční mikroskopie a metody zpracování obrazů pro sledování buněčné migrace. Experimentální nastavení pro mikrofluidní realizaci *"Scratch Wound Healing Assay"* s použitím trypsinu – EDTA pro vytvoření rýhy, a konfokálního mikroskopu Leica TCS SP8 X pro následující snímání pořízených dat bylo navrženo a otestováno s dostatečným počtem opakování. Vhodný algoritmus pro analýzu buněčné migrace byl napsán v programovacím prostředí Matlab. Závěrem této práce je diskuze získaných výsledků.

KLÍČOVÁ SLOVA

Kultivace savčích buněk, Scratch Wound Healing Assay, microfluidiní systémy, buněčná migrace.

ABSTRACT

This thesis describes the cell culture methods of mouse embryonic fibroblast (3T3), human umbilical vein endothelial (HUVEC), and Chinese hamster ovary (CHO) cell lines in microfluidic systems simulating capillary. Literature research for microfluidic realizations of *Scratch Wound Healing Assay* with fibroblasts and endothelial cell lines was performed in this thesis. The principles of confocal and fluorescence microscopy, and relevant image processing techniques used for quantifying cell migration were studied. Experimental setup for microfluidic *Scratch Wound Healing Assay* with using of trypsin – EDTA for creation of cell delusion, and confocal microscope Leica TCS SP8 X for subsequent image acquisition was proposed and tested. An appropriate algorithm for cell migration analysis was written in Matlab computing environment. Experiment's results are discussed in the conclusion of this thesis.

KEYWORDS

Mammalian cell culture, Scratch Wound Healing Assay, microfluidic systems, cell migration.

MORGAENKO, Katsiarina. Sledování migrace buněk v mikrofluidním systému metodou „Scratch Wound Healing Assay" [online]. Brno, 2019 [cit. 2019-05-16]. Dostupné z: https://www.vutbr.cz/studenti/zav-prace/detail/118995. Diplomová práce. Vysoké učení technické v Brně, Fakulta elektrotechniky a komunikačních technologií, Ústav biomedicínského inženýrství. Vedoucí práce Larisa Baiazitova.

PROHLÁŠENÍ

Prohlašuji, že svou diplomovou práci na téma Sledování migrace buněk v mikrofluidním systému metodou "Scratch Wound Healing Assay" jsem vypracovala samostatně pod vedením vedoucího diplomové práce a s použitím odborné literatury a dalších informačních zdrojů, které jsou všechny citovány v práci a uvedeny v seznamu literatury na konci práce.

Jako autor uvedené diplomové práce dále prohlašuji, že v souvislosti s vytvořením této diplomové práce jsem neporušila autorská práva třetích osob, zejména jsem nezasáhla nedovoleným způsobem do cizích autorských práv osobnostních a/nebo majetkových a jsem si plně vědoma následků porušení ustanovení § 11 a následujících zákona č. 121/2000 Sb., o právu autorském, o právech souvisejících s právem autorským a o změně některých zákonů (autorský zákon), ve znění pozdějších předpisů, včetně možných trestněprávních důsledků vyplývajících z ustanovení části druhé, hlavy VI. díl 4 Trestního zákoníku č. 40/2009 Sb.

V Brně dne ....

(podpis autora)

PODĚKOVÁNÍ

Rada bych poděkovala vedoucí diplomové práce páni Ing. Larise Baiazitové za účinnou metodickou, pedagogickou a odbornou pomoc, za její čas a ochotu, kterou mi věnovala při konzultacích v průběhu zpracování práce.

V Brně dne ....

(podpis autora)

Content

List of figures

List of tables

Introduction

The process of cell migration is involved in various aspects of biological mechanisms, such as immune response, wound healing, cancer metastasis and tissue development. Therefore, developing of reliable experimental methods is essential for studying underlying physiological and pathological processes on molecular scale. Scratch Wound Healing Assay is an in vitro technique, which allows to gain better understanding of the interplay of biological, chemical and physical factors affecting cell migration.

Conventional two-dimensional (2D) Scratch Wound Healing Assay is performed by creation of a cell delusion on confluent cell monolayer, with consequent observation of wound closure. However, conventional methods have some limitations, such as physical damaging of cells near the wound edges, along with an inability to generate and study the effects of growth factors and shear stress application. Conversely, in three-dimensional (3D) realization of Scratch Wound Healing Assay in microfluidics it is possible to overcome these shortcomings with use of fluid flow.

This thesis aimed to develop the experimental design of Scratch Wound Healing Assay using microfluidic device; to study a behavior of cell migration under constant flow; to create cell delusion using chemical influence of trypsin; test proposed experimental setup in order to proof the concept; examine cell migration rate and conclude whether this microfluidic version of Scratch Wound Healing Assay is a reproducible and reliable tool for a research.

For the purpose of this thesis cultivation methods of 3T3 and HUVEC lines in microfluidic devices were studied and tested. In vitro experiments analyzing chemical effect of trypsin to cell monolayer, persistence of cell monolayer labeling via fluorescent due within 24 hours, and consistency of laminar fluid flow in the microfluidic device Ibidi μ-Slide III 3in1 were performed. Based on achieved results, experimental setup for microfluidic realization of Scratch Wound Healing Assay using continuous trypsin flow for creation of cell exclusion was successfully tested. The subsequent image acquisition of the cell migration was fulfilled with confocal microscope Leica TCS SP8 X. After processing of obtained images, cell migration rate was analyzed as a closing of the wound over the time.

In conclusion a robust microfluidic platform and a set of software are described and characterized. This experimental setup for 3D Scratch Wound Healing Assay could be used in future studies, providing such advantages as precise control of the 3D biomimetic environment, excellent optical properties, and additionally enabling application of shear stress and generating

parallel flows. Thus, this thesis states that proposed realization of microfluidic Scratch Wound Healing Assay demonstrates a reliable and reproducible alternativity to conventional method.

.

1. Cell culture

Cell culture is the process, which involves the removal cells from their natural environment and subsequent growth in a favorable artificial condition. Within the broader context, cell culture refers to multicellular eukaryotes, plant tissue culture, fungal culture, microbiological culture, and used as a "cultivation medium" in virology. In the context of this thesis, cell culture refers to mammalian cells derived from a human or an animal, with following creation of in vitro environment. Favorable artificial condition is different for each cell type, but inherently consists of the necessary nutrients (amino acids, carbohydrates, vitamins, minerals), growth factors, hormones, gases (O_2, CO_2) and regulated physical-chemical environment (temperature, pH, osmotic pressure) to allow cells to proliferate. [1]

Today majority of the cell-based research is using 2D cell cultures in vitro. In adherent 2D cultures cells create a monolayer on flat and rigid substrates. Although 2D cell cultures has proven its reliability, there are limitations associated with 2D cultures, these included the disturbance of interactions between the cellular and extracellular environments, changes in cell morphology, polarity, and method of division. In contrast 3D cell cultures are able to mimic accurately the actual microenvironment, its structural architecture allows growth in all directions, thereby 3D cell culture realistically models tissue conditions and processes, thus providing with in vivo like responses. [2] [3] [4]

1.1 Sterile techniques

During in vitro experiments cells are mainly maintained in a suitable culture medium providing an environment applicable for their growth. Cultures are usually supplied in conical flasks, universal bottles or Petri dishes, the cotton wool plugs, screw caps or covers respectively serving to keep the cultures free of contamination from airborne bacteria or fungal spores. All glassware must be sterilized before use and sterile techniques should be observed throughout. Sterile techniques to prevent contamination are described by following rules:

- Maintain goof personal hygiene.

- Keep sterile work area, materials and reagents.

- Daily check for cell sample biological contamination.

- Cell transfers should be carried out as rapidly as possible, though without unnecessary haste and without the need of a partner to hold anything.

- Plugs and caps must be held in the fingers when temporarily removed from culture vessels and must be set down on the bench.

- Work in a laminar flow to ensure that airborne contaminants are carried upwards. [1]

1.2   Types and morphology of cell cultures

There are three major types of cell cultures, which include primary cell culture, secondary cell culture and cell line. Primary culture refers to the stage of the culture after the cells are dissociated from the parental tissue and proliferated in the appropriate environment until they become confluent. When a primary culture is passaged, it becomes known as secondary culture. After the first subculture, the primary culture becomes known as a cell line or subclone. A cell line may be finite or continuous depending upon whether it has limited culture life span, or it is immortal in culture. The passage number contains the information how many steps of subculturing the cells have undergone, thus it can be concluded for how long these cells have been in a culture.

Based on cells appearance and shape, their morphology, cells in culture can be divided into three basic categories: fibroblastic, epithelial and lymphoblastic (Fig. 1).
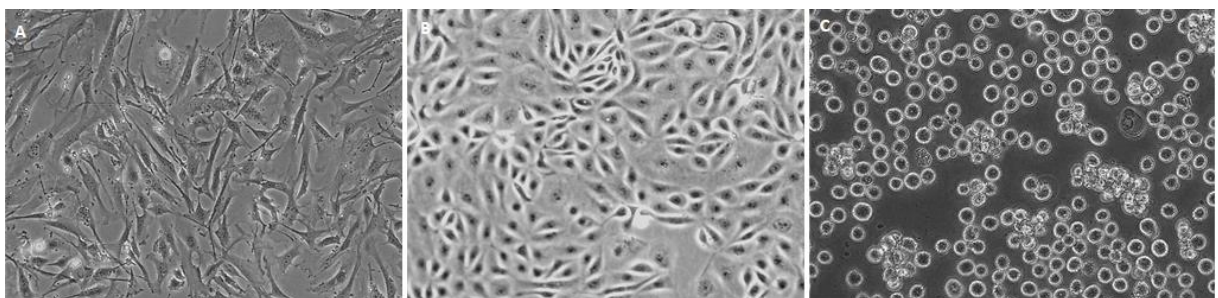
Figure 1: Types of mammalian cell morphology. A: fibroblastic morphology. B: epithelial morphology. C: lymphoblastic morphology. [5]

Fibroblastic morphology cell type includes cells that tend to be bipolar or multipolar with elongated shapes. Cells with epithelial morphology attain a polygonal shape with regular dimensions and grow attached to a substrate in discrete patches. Lymphoblastic cell type is usually spherical in shape and do not attach to the surface of the substrate. As a result, they are grown in suspension. [5], [6]

1.3   Materials and reagents

In practical part of this thesis were used following materials and reagents as: Dulbecco's Modified Eagle Medium (DMEM), Endothelial cell growth medium (EGM-2), Nutrient Mixture F-12 Ham, Phosphate Buffered Saline (PBS), Fetal Bovine Serum (FBS), Trypsin – EDTA (ethylenediaminetetraacetic acid), 3T3 (3 day transfer, inoculum 3×10^5 cells) cell line, Human Umbilical Vein Endothelial Cell (HUVECs), Chinese hamster ovary (CHO) cell line.

Culture medium is a solid, liquid or semi-solid designed to support the growth of microorganisms or cells. Culture medium contains all the most needed elements for growth, supplied with form of organic carbon for energy, a source of nitrogen for protein and vitamin synthesis, and several minerals. Medium need for certain cell lines depends on cell origin and innate function. In further progress were used DMEM, EGM-2 and Nutrient Mixture F-12 Ham types of media. DMEM interpreted as Dulbecco's Modified Eagle Medium is medium modification contains high concentration of amino acids and vitamins, as well as additional supplementary components. EGM-2 or Endothelial Cell Growth Medium is an extract of bovine neural tissue containing growth promoting factors for vascular endothelial cells of mammalian origin. Nutrient Mixture F-12 Ham is used for growth of primary rat hepatocytes and rat prostate epithelial cells, including CHO cells. [7]

PBS is a balanced salt solution used for a variety of cell culture applications, such as washing cells before dissociation, transporting cells or tissue, diluting cells for counting, and preparing reagents. [7]

FBS is commonly used as a supplement to basal growth medium in cell culture, because of its high content of embryonic growth promoting factors. In cell culture, serum provides a wide variety of macromolecular proteins, low molecular weight nutrients and other compounds necessary for in vitro growth of cells, such as hormones and attachment factors. Serum also adds buffering capacity to the medium and binds or neutralizes toxic components. [7]

Trypsin – EDTA is an irradiated mixture of proteases derived from porcine pancreas. Due to its digestive strength, trypsin is widely used for cell dissociation, routine cell culture passaging, and primary tissue dissociation. The trypsin concentration required for dissociation varies with cell type and experimental requirements. [7]

3T3 cell line is mouse embryonic fibroblast cells that were cultured by the designated so-called "3T3 protocol". Protocol's designation refers to the abbreviation of "3 day transfer, inoculum 3×10^5 cells", which means cells were transferred every 3 days and inoculated at the

rigid density of 3×10^5 cells per 25 cm² dish continuously. With their ability to liberate growth factors, lay down fibroelastic matrices, and proliferate at sites of inflammation, fibroblasts are considered to be among the relatively easy to grow cell lines and play critical roles in studies for a range of mechanistic and cell-based assays, including protein functional analysis, wound healing, tissue repair, and remodeling. According to the 3T3 cell culture protocol, cell layer become confluent at a density of approximately 4×10^4 viable cells $\cdot$ cm^{-2}. DMEM medium formulated with the addition of 10 % FBS is suitable solution used for 3T3 cells culturing. Flasks should be incubated at 37 °C in 5 % CO_2. For the avoidance of cells senescent there is a need to realize process of subculturing every 3-4 days, when cell layer reaches confluence, and renew complete medium 2 times a week. [8]

HUVECs are cells derived from the endothelium of veins from the umbilical cord. HUVECs play a significant role as a model system to study many aspects of endothelial function and disease, such as oxidative stress, hypoxia and inflammation related pathways in endothelia under normal or pathological conditions and the role of the endothelium in the response of the blood vessel wall to stretch, shear forces, and the development of atherosclerotic plaques and angiogenesis. Referring to the HUVEC culture protocol cell layer become confluent at a density of approximately 8×10^3 to 3×10^4 viable cells/cm². A high-quality EGM-2 medium prepared from bovine neural tissue should be used to propagate HUVECs line during culturing. Flasks should be incubated at 37 °C in 5 % CO_2. Growing cell line has an estimated doubling time of 5 to 6 days. Cultures should be fully fluid changed every 48 hours. [9]

CHO cells have demonstrated several advantages to make them preferred mammalian cell line for purposes of biomedical research. One of them is an ability to adapt and grow in suspension culture, another one is a capability of growing in serum-free chemically defined media. According to CHO cell culture protocol, culture should be 50 to 80% confluent to ensure that the cells are actively growing. When viable cell density reaches 1 x 10^6 cells/ml it is suggested to passage cells at 5 x 10^5 cells/ml. Once cell density reaches at least 1 x 10^6 cells/ml with a viability of at least 90%, the cells may be considered adapted to suspension culture, with seeding density reduced to 2 x 10^5 to 3 x 10^5 cells/ml. Cell samples should be stored at 37 °C in 5 % CO_2. CHO cells undergo one duplication within the period of 20-24 hours. [10]

2. Cell migration

Cell migration is fundamental cellular process, which characterizes cell movement in response to chemical or mechanical signal. There are two types of cell migration - single cell migration and collective cell migration. As in practical part of this thesis were used 3T3 cells, CHO and HUVECs, this chapter is looking into migration mechanisms of fibroblasts and endothelial cells. Mechanism of single-cell migration includes such steps as:

1.   Extension: actin filaments at the leading edge stretch in the direction of protrusive force.

2.   Adhesion: new focal adhesion points are rapidly linked to the network of actin filaments.

3.   Translocation: combined activity of actin movement and contractile forces generates tension to pull the cell body forward.

4.   De-adhesion: forces produced by the contractile network combined with actin filament and focal adhesions disassembly help to retract the trailing cell edge. [11]

Fibroblast-type cells are a good example of single-cell migration (Fig.2 B). Fibroblasts play a very important role in wound healing process, as in vivo they are usually present in connective tissue. However, when compare single fibroblast migration in vitro and in vivo conditions, cells will have varying speed and morphology. In vitro, fibroblasts move slowly with an average speed less than 1 im/min and often change its direction. Numerous studies have shown that while fibroblasts are migrating into a wound, they tend to have a large lamellipodium extending into the wound with few stress fibers in the cell; on the other hand, stationary fibroblasts have smaller lamellipodia, and are characterized by multiple stress fibers (Fig.3). At the same time, fibroblast migration morphology is quite different in 2D and 3D environments. In 2D cell culture, fibroblasts have large lamellipodia and filopodia then in 3D models. Described properties are applicable to 3T3 fibroblast-type cell line. [12]
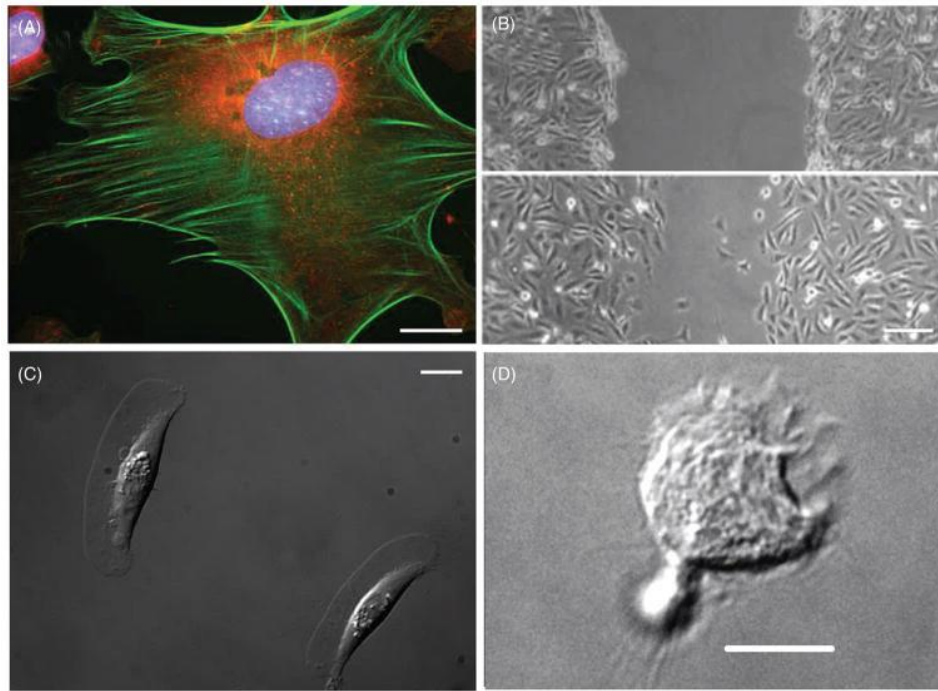
Figure 2: Cell migration types: A) A stationary stained fibroblast cell (blue – DNA, red – mitochondria, green – actin filament), scale bar 10 μm. B) Fibroblasts migrating into wound. Top: wound after creation of cell exclusion, bottom: fibroblast migration after 15 hours, scale bar 100 μm. C) Migrating zebrafish fibroblast-type cells with large lamellipodia scale bar 10 μm. (D) Migration human promyelocytic leukemia cell on a glass substrate, scale bar 10 μm. [12]
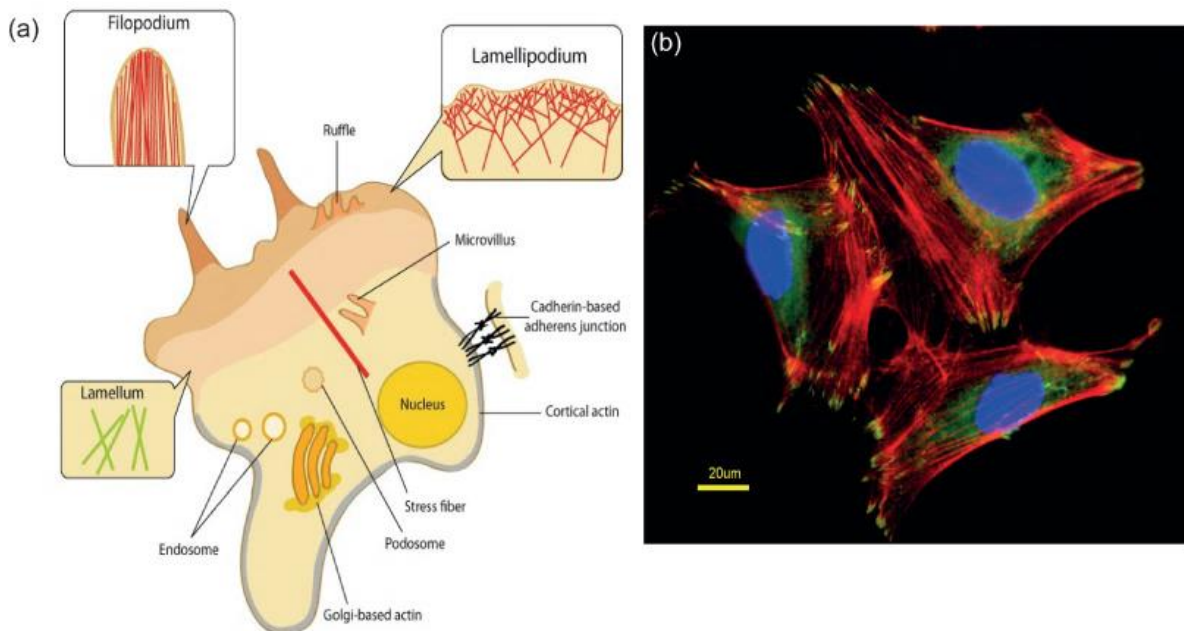
Figure 3: (a) Schematic representation of a cell attached on a substrate. Actin filaments: filopodium, lamellipodium and lamellum, where lamellipodia, lamellae and ruffles appear sheet-like, whereas filopodia finger-like. (b) Immunofluorescent image of a fibroblast showing the different adhesive structures (in red, actin filaments in green, nucleus in blue blue – DNA, red – focal adhesions, green – actin filament), scale bar 20 μm. [11]

Collective cell migration is a migration type, where cells represent a moving group. This migration type uses similar mechanisms as single cells to protrude, polarize, contract, and adhere. However, their ability to interact with each other both chemically and mechanically enables additional migration mechanisms (Fig.4). [12]

Endothelial cells migration varies depending on the context. Cells migrate individually, in chains or sheets; this process is modulated by the environment. [13]
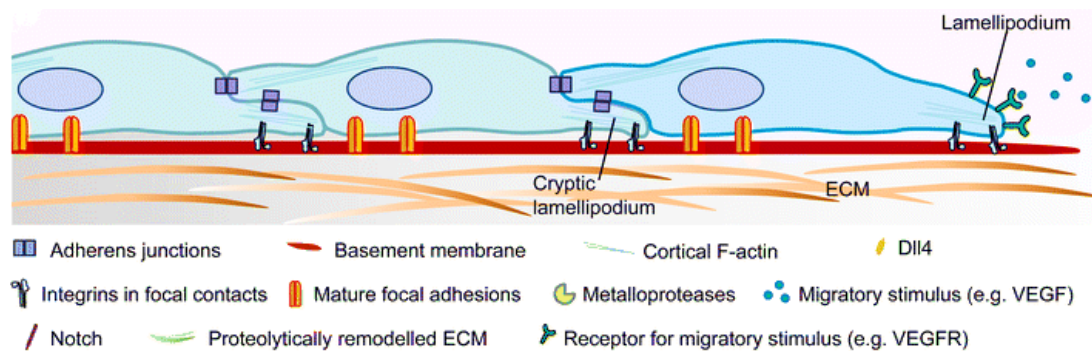
Figure 4: Collective endothelial sheet migration. When migratory stimulus is recognized leader cell (blue) forms a lamellipodium and new focal contacts. The following cells (green) are characterized by cryptic lamellipodia. [13]

At the same time, endothelial migration mechanism is different in 2D and 3D environments. When endothelial cells are presented to 2D environment, they predominantly migrate as tightly associated epithelial sheets. In 3D environment, cell detached from their origins migrate as isolated groups or clusters of cells. Additionally, in 3D leading cells form filopodia or pseudopodia instead of flat lamellipodia in 2D. [13]

Previous study has shown, that for HUVECs cell migration rate in 3D environment is 12 μm/h, and 25 μm/h in 2D environment, and 3T3 cells migrate with the speed of 18 μm/h and 29 μm/h, in 2D and 3D environments respectively. [12]

3. Scratch wound healing assay

The scratch wound healing assay is a technique to measure cell migration in vitro. Wound healing assays use cells derived from either cell lines or primary isolations from blood or tissue. The basic steps involve culturing a confluent cell monolayer and creating a cell exclusion either by removing a growth barrier or by damaging the cell layer. Damage may have mechanical, thermal or chemical character. The exposure to the cell-free area induces the cells to migrate into the gap. This process is captured via imaging at the beginning and at regular time intervals (Fig.5). The subsequent image acquisition of the wound closure provides information about the migration characteristics. The in vitro scratch wound healing assay is powerful tool for studies on the effects of cell–matrix and cell–cell interactions on cell migration, mimic cell migration during wound healing in vivo and are compatible with imaging of live cells during migration to monitor intracellular events if desired. [14]
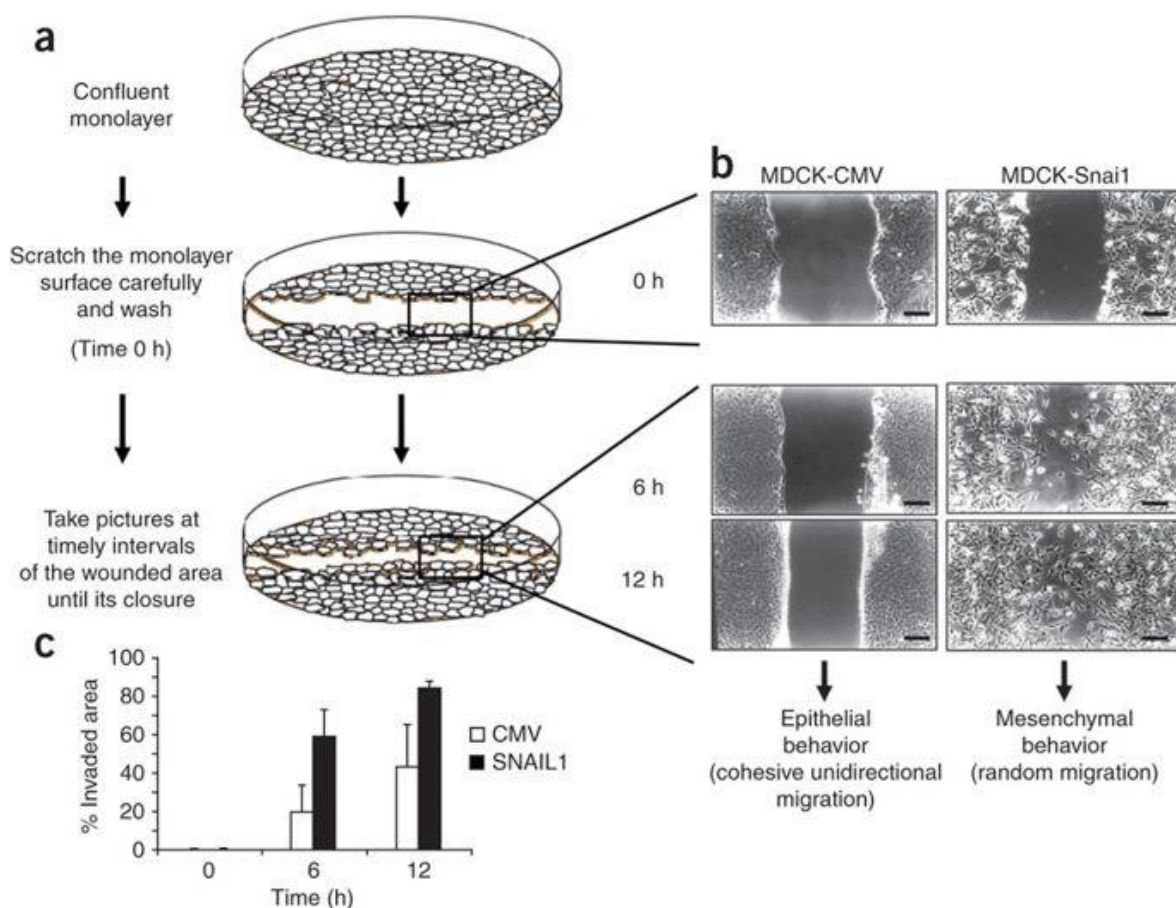
Figure 5: (a) Schematics description of scratch assay. (b) Phase contrast images of the cultures taken at 0h (immediately after scratching), and at the indicated time intervals (6h, 12h) showing the wound closure by cells migration in a random manner (right panels) and as a cohesive sheet (left panels). [15]

3.1   Cell exclusion

In collective cell migration assays cell exclusion or also cell depletion is a cell-free gap created in a cell monolayer. There are few ways to create cell exclusion:

- Direct manipulation: is provided by destroying of monolayer through mechanical, electrical, thermal or chemical influence.
- Physical exclusion: is realized by placing barrier (plastic insert, liquid or gel) to the cell culture plate. [14]

All of techniques described above have different pros and cons. In this study, cell exclusion was created with application of trypsin. Trypsin mechanism concludes in cutting amino acids on their C-terminus. In cell culture it works as cutting away adhesions which are attaching cell layer to the culture dish. Most trypsin solutions for cell culture contain ethylenediaminetetraacetic acid, which acts as a chelator for calcium. By removing calcium from a solution with cells, cadherins which hold cells to each other, are broken and cells separate from each other as well as from the surface of the tissue culture plastic, thus cell-free gap is created. [16]

3.2   Realization of Scratch Wound Healing Assay in a microfluidic device

Microfluidics is a technology of manipulating and detecting fluids in the micro scale. A microfluidic device can be identified by the fact that it has one or more channels with at least one dimension less than 1 mm. The majority of microfluidic-based wound healing assays use the multiple laminar flows in microfluidic channels to selectively remove cells enzymatically, generating the wound with a clear boundary and monitoring corresponding cell migration.

Key articles for this thesis describe different ways of fabrication a microfluidic device for cell migration in wound healing assay.

Fig. 6 schematically described device design and wound healing assay procedure, where Yuanchen *et al*. created PDMS (polydimethylsiloxane) microchannel with dimensions of 3 mm in length, 0.8 mm in width. Three microchannel ports (two channel inlets and one outlet) with a diameter of 5 mm were designed to facilitate liquid droplet manipulation.
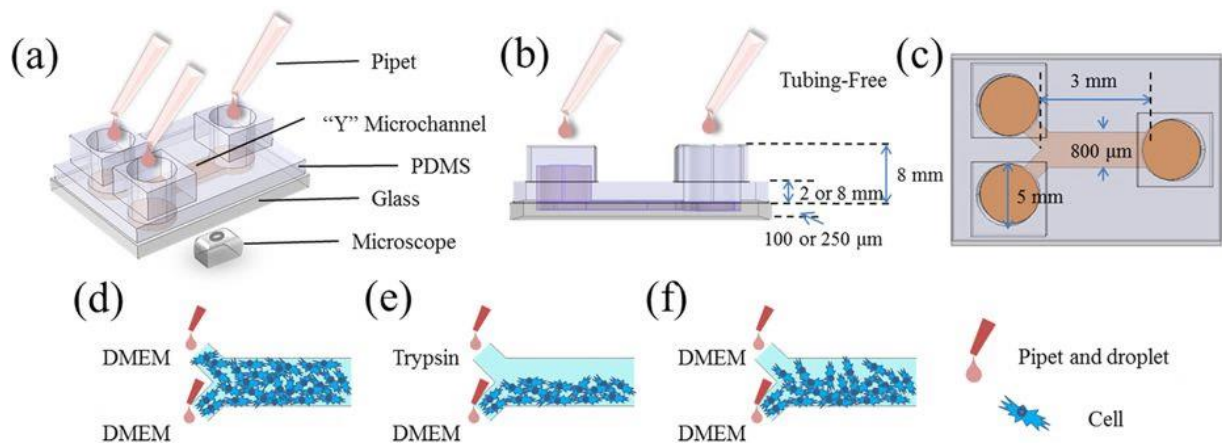
Figure 6: (a–c) Schematic of the tubing-free microfluidic wound-healing assay quantifying cell migration. (d), wound generation (e) and cell migration monitoring (f). [17]

The fabricated microfluidic device was sterilized under ultraviolet overnight, followed by surface coating of fibronectin by flushing into the microfluidic device using micro pipets and kept within the microfluidic channels overnight. Then, the coating solution was removed by aspiration and the channels were rinsed with culture medium. After culture medium solution was removed and replaced with cell suspension solutions of 20 μl at two inlets and 30 μl at the outlet (5 million cells per ml). Supplemented culture medium was replaced every 12 hours where solutions in three ports were removed and replaced with 60 μl fresh supplemented culture medium each. In this study, gravity was used as the driving force to regulate fluid flow, enabling the wound generation without the requirement of external pumps and tubing. Trypsin solution and the supplemented culture medium were applied at two channel inlets to generate the wound. Following the wound generation, the trypsin solution was replaced with culture medium supplemented with different chemokines and the microfluidic device was transferred to the incubator. Subsequent image acquisition was performed at timepoints 0 hour, 3 hour, 6 hour, 12 and 24 hours. Average cell migration distance at each timepoint was analyzed via NIH ImageJ image analysis software. In this article authors refer to the previous study by Nie *et al.*, where fabricated PDMS microfluidic model with analogous geometrical parameters and application of trypsin for wound creation was successfully used. The difference consists in the cell line, which was used for migration study. Schematic illustration of mutual experimental concept is shown on Fig.7. [17], [18]
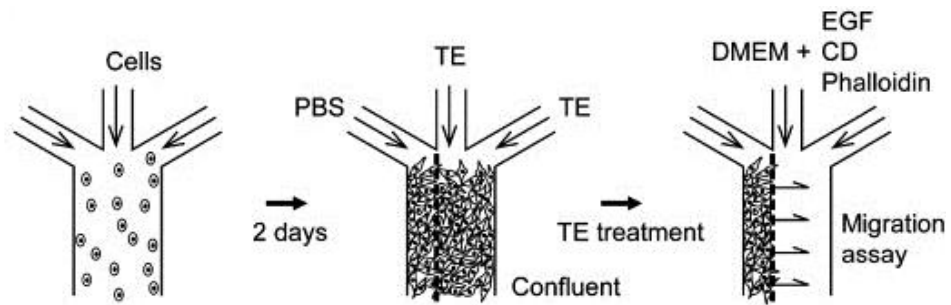
Figure 7: Patterning processes to create wound edges for the confluent cells sheet formed in the microchannel. [18]

Similar model is introduced in the article by van der Meer *et al.,* where microfluidic channels of PDMS had the inverse shape of a long channel with dimensions 60 μm×500 μm×2 cm (height×width×length) separated on one side into three smaller inlet channels. The microfluidic channels were coated for 2 hours with fibronectin solution and then flushed with EGM-2 medium. Prepared cell suspension with density $20 \cdot 10^6$ viable cells/ml was pipetted into the channel, after which the microfluidic devices were overlaid with EGM-2 and incubated at 37°C and 5% CO_2. To prepare a cell exclusion in the microfluidic channel, each of the three inlets was connected to its own 5-ml syringe. Two of the syringes contained endothelial basal medium with 2% fetal bovine serum, and the middle syringe contained trypsin solution. The contents of these syringes were pushed through the microfluidic channel at a total rate of 3 ml/h for 15 min. After this, the pump was stopped, the channels were flushed with EBM-2 and 2% FBS, and placed in the incubator. When wounds were prepared in the conventional wound-healing assay, a single scratch was made in the endothelial monolayer using a micropipette tip. Subsequently, the cells were washed once with PBS and then incubated with EBM-2, 2% FBS at 37°C, 5% CO_2. Images of wound closure were taken at timepoints 0.5 hour, 2 hour, 6 hour and 18 hour. Cell migration was measured as the distance from the initial leading wound-edge to the position of the migration cells. Experimental setup is described on Fig. 8. [19]
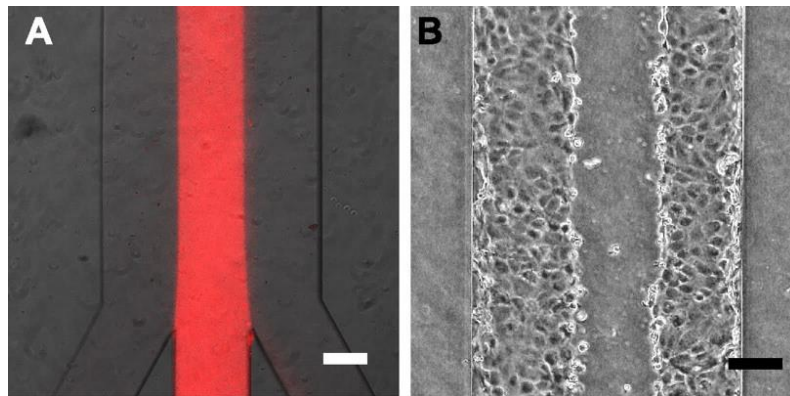
Figure 8: (A) fluorescent micrograph of a fluid stream shows that no visible mixing of parallel fluid streams occurs in the microfluidic channel. Scale bar, 100 μm. (B) A wound that was prepared by treating an endothelial monolayer with parallel trypsin-containing fluid flow in a microfluidic device. Scale bar, 100 μm. [19]

The next microfluidic model proposed by Sticker *et al.* describes differ mechanism of lab-on-chip realization wound healing assay in microfluidic device (Fig. 9). Two microdevices containing integrated pneumatically activated actuators were designed for either cell depletion, using a flexible membrane, or cell exclusion, using an integrated microstencil. Both devices consisted of three layers: a top pneumatic layer, a middle flexible PDMS membrane, and a microchannel network bottom layer. In the pneumatic layer, a 1.5 and 2.5 mm diameter circular shaped frame for cell depletion and cell exclusion was placed in the middle of the four 90 μm high, 2.5 mm wide, and 7.5 mm long cell culture chambers. Microchambers were rinsed by PBS and loaded with a protein mixture comprising 10 μg/ml fibronectin and 5 μg/μl fibrinogen and then placed on a heating plate (37 °C) to ensure temperature stability. Prior to experimentation, the microchip was disinfected using 70 % ethanol and washed with PBS prior to coating with a 1 % gelatin solution for 1 hour. Then, prepared cell suspension was gently loaded into microchannels. Following a cell adhesion period in the absence of fluid flow, a constant medium perfusion of 3 μl/min was applied using a syringe pump. As soon as a confluent cell layer (typically 1 to 2 days) was obtained, a circular wound was mechanically induced by pneumatic actuation of the PDMS membrane. Bending was induced by rapidly increasing the pressure load to 150 kPa (differential pressure) and then immediately releasing to 0 kPa using a pressure controller. The medium perfusion was kept on while mechanical damage was being performed. [20]
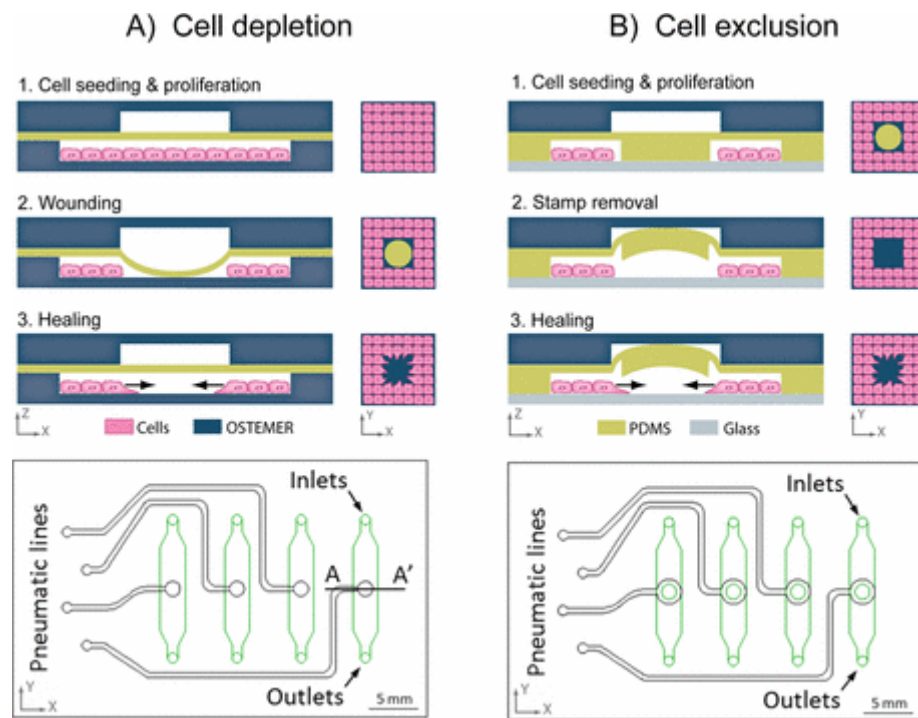
Figure 9: Schematic illustrations of the functional principles and pictures of (A) the cell depletion and (B) the cell exclusion microdevice showing the chips cross sectional view on the top. The mask designs with an overlay of pneumatic (black) and fluidic (green) layer in the middle, and a representative image of the devices on the bottom. Scale bar, 5 mm. [20]

3.3   Influential factors

To summarize all measures tooled in the research described above there are few major influential parameters needed to focus attention on.

- The number of the cell passage. To avoid cells senescence, it is reasonable to use cells which are between passage 2 and 8.

- When seeding cells for a migration assay, it is important to cover the total culture area. If the cell density is too low, cell migration rate will be affected.

- Integrity of the monolayer. Cells grow in tight monolayers with extensive cell-cell contacts. These cell-cell contacts are important to provide signaling and functioning. It is therefore important that the cells have formed a confluent monolayer with tight cell-cell contacts before migration in a wound-healing assay is assessed. The integrity of the monolayer can be checked by staining for specific cell adhesion molecules. (Fig. 10).
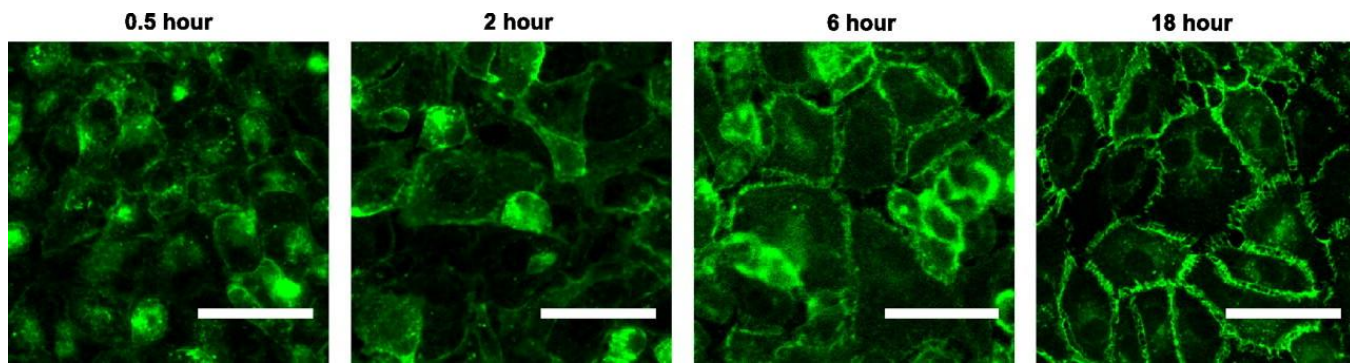
Figure 10: Fluorescent staining for vascular endothelial cadherin at different time points after seeding. Scale bars, 50 μm. [19]

- Affecting cell migration with growth factors. Migration rate depends on presence of biochemical factors.

- Shear stress impact. Applying a shear stress leads to a significant increase in migration rate. Moreover, cell morphology during migration is different. Cells migrate into the wound along with the direction of the applied shear stress.

- Effect of channel geometries. Geometry of the channel has to guarantee suitable regulation of the diffusion of oxygen, which can further affect cellular properties including cell growth and migration.

- Affecting cell migration with coating of microfluidic channel. Favorable coating can provide a better environment to promote the migration. [18], [19]

- Laminar flow conditions should be ensured for Scratch Wound Healing Assay realization in microfliud flow system.

3.4   Advantages and limitations

The two most widely used assays for quantification cell migration are the Boyden chamber assay and the wound-healing assay.

The microfluidic version of the assay has some unique advantages compared with its conventional counterpart (Boyden chamber). Because of the small size, small amounts of cells and reagents are needed. Furthermore, the microfluidic wound-healing assay may be combined with other microfluidic analysis tools in the same device, the so-called "lab on a chip" concept. Another advantage of the microfluidic wound-healing assay is that it is compatible with high-magnification microscopy. Moreover, stable and tunable gradients of growth factors and drugs can be generated, and physiologically relevant shear stresses can easily be produced while studying migration.

Using a Boyden chamber assay, cell migration with presence of gradients of can be also quantified. However, in this assay, it is impossible to control the shape of the gradient or to visualize cells as they migrate into the gradient. The main advantage of the Boyden chamber assay compared with the wound-healing assay is that gradients of soluble factors can be generated by adding those factors to only one of the two compartments.

There are several disadvantages and limitations of the in vitro scratch assay compared to other available methods. It does not replace other well-established methods for chemotaxis such as the Boyden chamber assay, as no chemical gradient is established. It takes a relatively longer time to perform than some other methods. One to two days are needed for the formation of cell monolayer and then 8–18 hours for cell migration to close the scratch. Relatively large number of cells and chemicals will be required for the assay as it is usually performed in a tissue culture dish. Therefore, it is not a method of choice if the availability of cells or chemicals is limiting. Despite these limitations of the method, overall, in vitro scratch assay is still often the method of choice to analyze cell migration in a laboratory because it is easy to set up, does not require any specialized equipment and all materials required for the assay are available in any laboratory that performs cell culture. [17], [18], [19]

4. Microscopy

Microscopy is essential and major analytical tool used to monitor cell physiology. Microscopy offers different techniques to view objects and areas of objects that are not within the resolution range of the normal eye.

4.1   The fluorescence fundamentals

Fluorescence is the emission of light by a substance that has absorbed light or other electromagnetic radiation. Fluorescent effect is the result of a three-stage process that occurs in molecules called fluorophores or fluorescent dyes. A fluorescent probe is a fluorophore designed to respond to a specific stimulus or to localize within a specific region of a biological specimen. The process responsible for the fluorescence is illustrated by Jablonski diagram (Fig. 11). [21]
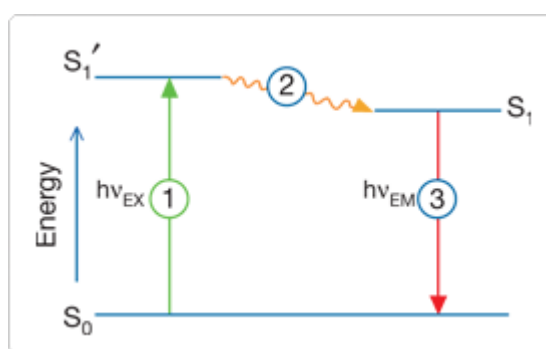
Figure 11: Jablonski diagram illustrating the processes involved in the creation of an excited electronic singlet state by optical absorption and subsequent emission of fluorescence. The labeled stage 1 is excitation, when a photon is supplied by an external source, and absorbed by the fluorophore; S1' an excited electronic singlet state; 2 is excited-state lifetime stage, when the fluorophore undergoes conformational changes; S1 is a relaxed singlet excited state; stage 3 is the stage of fluorescence enmission; S0 is the ground stage. [21]

The fundamental fact to the high sensitivity of fluorescence detection techniques is that a single fluorophore can generate many thousands of detectable photons. The fluorescence excitation spectrum of a single fluorophore species in is usually identical to its absorption spectrum. The absorption spectrum can therefore be used as an excitation spectrum data set. Under the same conditions, the fluorescence emission spectrum is independent of the excitation wavelength, due to the partial dissipation of excitation energy during the excited-state lifetime (Fig.12). The emission intensity is proportional to the amplitude of the fluorescence excitation spectrum at the excitation wavelength. [21]

22
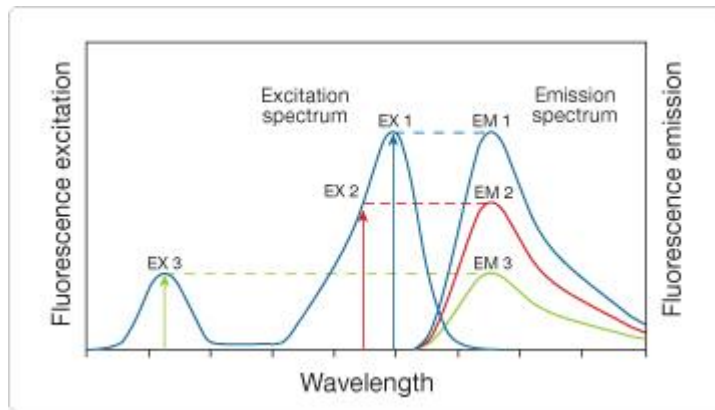
Figure 12: Excitation of a fluorophore at three different wavelengths (EX 1, EX 2, EX 3) does not change the emission profile but does produce variations in fluorescence emission intensity (EM 1, EM 2, EM 3) that correspond to the amplitude of the excitation spectrum. [21]

4.2   Fluorescent dyes

Fluorescent dyes or fluorophores are fluorescent tools for cell biology that have been conjugated to various molecules to give them a certain function or allow them to label specific organelles. Using fluorophores provides greater contrast compared with brightfield microscopy and allows to visualize different structures or proteins within a cell in the same experiment. Fluorophore can be produced in a plenty of different forms, each chemical modification with a different specificity (Fig.13). [22]
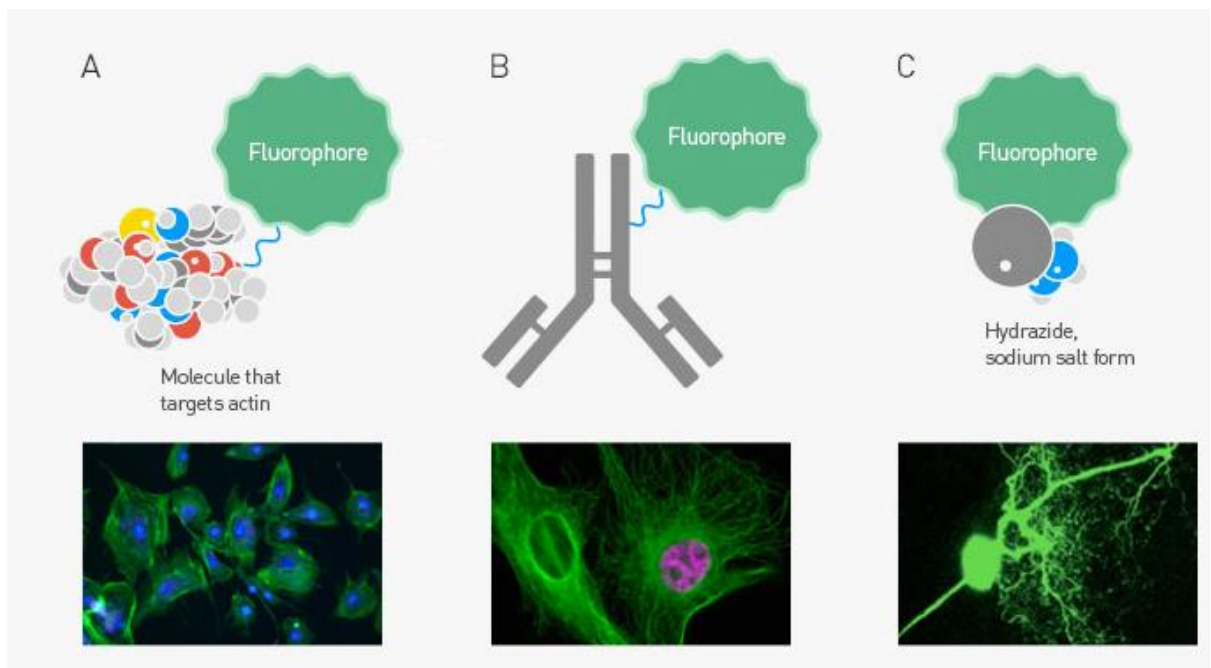
Figure 13: A single fluorophore can be modified to carry out any number of labeling jobs, including functionalized forms for labeling cell structure components such as actin (A) and tubulin (B) and salt forms for whole-cell staining (C). [22]

23

For experimental part of this thesis Calcein AM (Calcein-acetoxymethylester) and CellTracker™ Green CMFDA (5-chloromethylfluorescein diacetate) were chosen for fluorescent cell labeling due to their compatibility with 3T3 cell line, CHO and HUVECs.

Calcein AM is a non-fluorescent, cell permeant compound, which is converted by intracellular esterase into calcein, an anionic fluorescent form. Calcein AM is used in microscopy to provide both morphological and functional information of viable cells. The excitation and emission wavelengths of Calcein AM are 495 nm and 516 nm, respectively (Fig.14). [23]
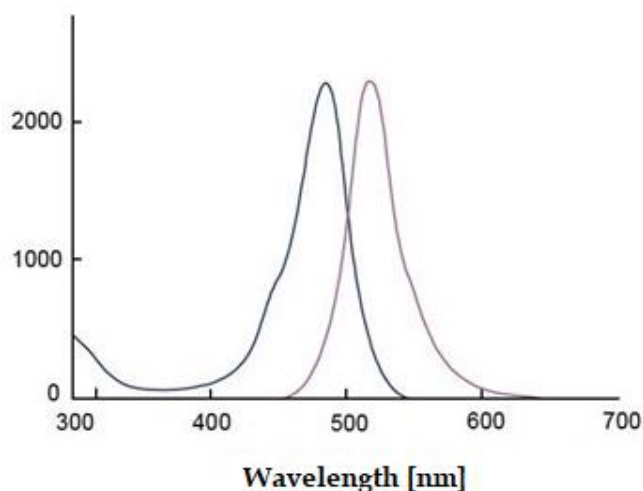
Figure 14: Calcein AM fluorescent specters. [23]

CellTracker™ Green CMFDA is a fluorescent dye for multigenerational monitoring of cell movement or location. It's green 492 nm excitation and 517 nm emission spectra are ideal for multiplexing with red fluorescent dyes and proteins. According to technical protocol provided by Thermo Fisher Scientific CMFDA has low cytotoxicity, does not affect viability or proliferation with signal retention of >72 hours.

4.3 Fluorescent microscopy

The fluorescent microscopy is based on the phenomenon that certain material emits energy detectable as visible light when irradiated with the light of a specific wavelength. The basic task of the fluorescent microscope is to let excitation light emit the specimen and then sort out the much weaker emitted light to create the image. Fluorescent microscope has a filter that only lets through radiation with the desired wavelength that matches scanning fluorescing material. The radiation collides with the atoms in specimen and electrons are excited to a higher

energy level. When electrons relax to a lower level, they emit light. In a second filter emitted light is separated from the brighter excitation light to become visible. [24]

4.4 Laser-scanning confocal microscopy

All the major concepts of fluorescence excitation and emission also apply to laser-scanning confocal microscopy. A bright point excitation source – laser and a sequential scanning method of the point source of illumination are major differences. The goal of confocal microscopy is to reject out-of-focus light from the image. This is achieved with a pinhole aperture that ensures that light reaching the detector comes only from the confocal point in the specimen where the excitation light was focused (Fig.15). By scanning the confocal excitation and detection point across the specimen, an image can be sequentially compiled, pixel by pixel, by recording the fluorescence intensity at each position. [25]
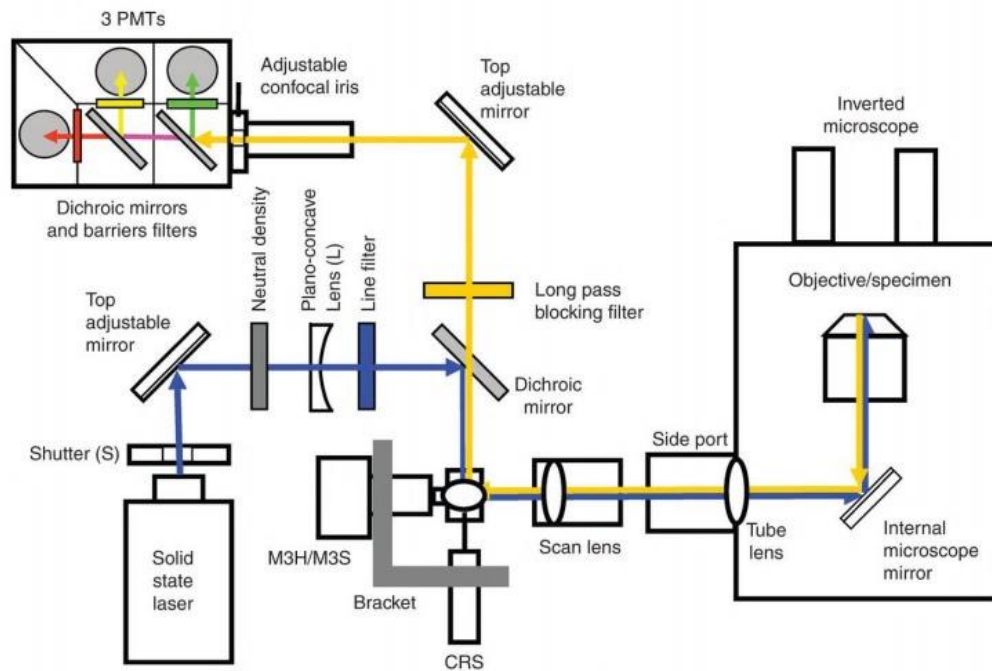
Figure 15: Basic elements of a laser scanning confocal microscope. Laser light is directed to the scan mirrors via a dichroic mirror. The laser is scanned across the specimen by the scan mirrors and the returning emitted fluorescence is descanned by the same mirrors and transmitted by the dichroic mirror. The fluorescence passes through the barrier filter and is focused on to the pinhole before reaching the PMTs. Additional dichroic mirrors can be used to separate fluorescence wavelengths. [25]

4.5 Leica TCS SP8 X

In practical part of this thesis the subsequent image acquisition was realized by using laser-scanning confocal microscope Leica TCS SP8 X.

The Leica TCS SP8 X is equipped with two sensitive HyD detectors, one Photo-multiplier Tube (PMT) detector for fluorescence and an additional PMT for bright-field imaging. Leica TCS SP8 X is equipped with white light laser. Images can be acquired with scan resolutions of up to 8192×8192 pixels. Spectral detectors permit independent real-time adjustment in the range from 380 nm to 800 nm for each of the confocal fluorescence detector channels. Images can be acquired in simultaneous or sequential scan modes. [26]

5. Digital microscopic images processing

Digital image processing is essential tool used in biomedical research. Digital microscope image processing is used to extract, count, locate, and measure attributes information presented in a microscope image. This chapter describes concepts, which were used for an analysis of the obtained microscope images.

General digital image processing system includes image acquisition, image digitalization, preprocessing and image analysis steps. Image enhancement is a preprocessing step which can includes noise suppression, contrast adjustment, band-pass filtering, detail enhancement by image sharpening, geometrical transforms, edge representation, etc. Output of the enhancement processing is an input image with improved appearance. Image analysis follows preprocessing step. As per application requirement various image processing techniques can be used for image analysis. Morphological image processing, image segmentation, object measurement and object classification methods are widely used techniques for microscope image analysis. [27]

5.1 Image processing fundamentals

Image histogram is a plot of pixel counts belonging to different intensity levels, which provides information of the distribution of intensity levels in the image (Fig.16).
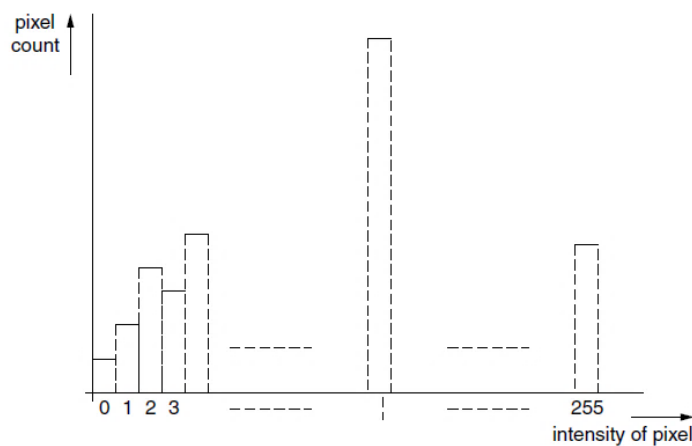
Figure 16: Schematic plot of a histogram of an image with a single-byte pixel representation. [28]

Information of pixel frequencies may serve to assess the adjustment of the imaging system with respect to utilizing the available dynamic range of pixel values. The value of a pixel is its intensity. The intensity of an image could refer to a global measure of that image, such as mean pixel intensity. A relative measure of image intensity could be how bright (mean pixel intensity) the image appears compared to another image. An edge in an image is a curve that

follows a path of rapid change in image intensity. Edges are often associated with the boundaries of objects in a scene.

2D median filter is a nonlinear operation, which selects the middle term of the sequence in two dimensions as the output (Fig. 17). Since image edges tend to correlate spatially across multiple scales whereas noise does not, median filter is more effective than convolution when the goal is to simultaneously reduce noise and preserve edges.
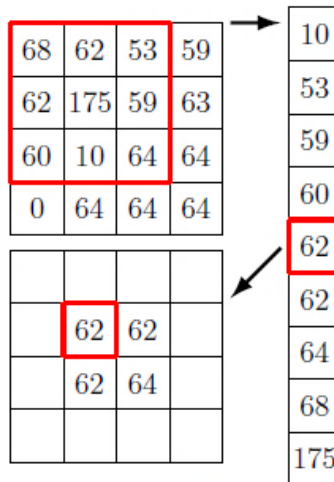
Figure 17: Schematic illustration of median filter. [29]

Top-hats and bottom-hats are operators defined as differences between the original image and one of the morphologically derived images. Top-hat filtering computes the morphological opening of the image and then subtracts the result from the original image. Bottom-hat filtering computes the morphological closing of the image and then subtracts the original image from the result (Equation 1,2).

$$T_H(x) = (x) - O_H(x) \tag{1}$$

$$B_H(x) = C_H(x) - (x) \tag{2}$$

Where (x) is an original image, $O_H(x)$ is an operation of opening applied to the original image, $T_H(x)$ is a difference between original image and derived image of morphological opening. $B_H(x)$ is a difference between original image and derived image of morphological closing $C_H(x)$. [28], [29]

Morphological structuring element is an inherent parameter of morphological operations. Multidimensional structure element is determined as a matrix that identifies the pixel in the image being processed and defines the neighborhood used in the processing of each pixel (Fig. 18).
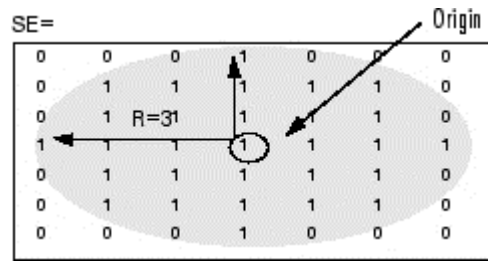
Figure 18: Multidimensional structure element 'disk', with radius R=3[1]. Ones represent pixels included in the morphological computation, and zeros are excluded. Origin is the center pixel of the structuring element being processed. [30]

Morphological operators are classified as non-linear operators. An image and a structuring element (SE) is are used as an input. If input image is a grayscale image, the intensity value is taken to represent height above a base plane, so that the grayscale image represents a surface in 3D Euclidean space. Then the set of coordinates associated with this image surface is simply the set of three-dimensional Euclidean coordinates of all the points within this surface and all points below the surface, down to the base plane. Other operators can be derived as a combination of them. Structuring element or matrix mask is a set of point coordinates, which has characteristics of its shape encoded, this mask is shifted over the image and at each pixel of the image its elements are compared with the set of the underlying pixels. The basic morphological operators are erosion and dilation. Erosion operator erode the boundaries of regions of foreground pixels (white pixels) of an input image (Fig.19). Thus, areas of foreground pixels shrink in size, and holes within those areas become larger. In contrast, dilatation operator gradually enlarge the boundaries of regions of foreground pixels on an input image (Fig.20). Therefore, areas of foreground pixels grow, simultaneously with holes within those regions become smaller. Opening operator is determined as an erosion followed by a dilation using the same structuring element for both procedures. Opening operator tends to preserve foreground regions, which have a shape of the structuring element, simultaneously eliminating all other regions of foreground pixels. Closing operator is defined as a dilation followed by an erosion using the same structuring element for both operations. Closing operator preserve background regions of an input image, which have a similar shape to this structuring element, while eliminating all other regions of background pixels.
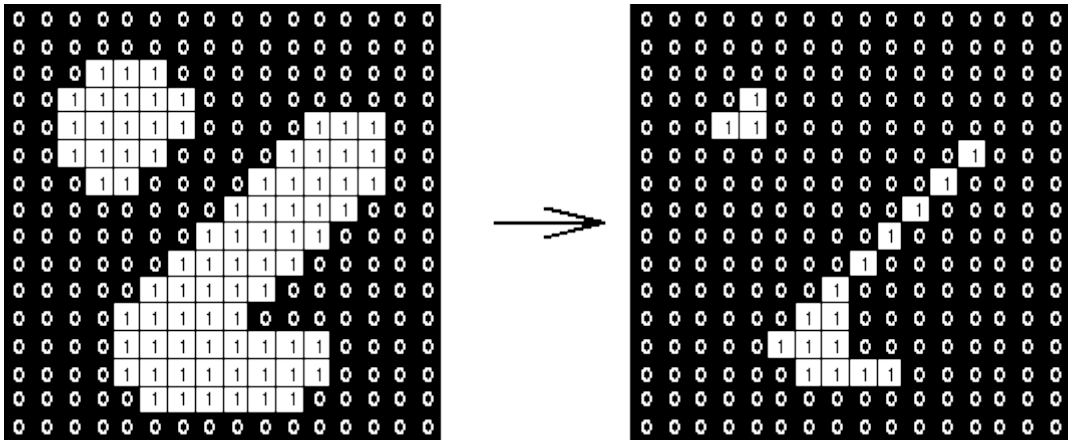
Figure 19: Effect of erosion using a 3×3 square structuring element. [30]
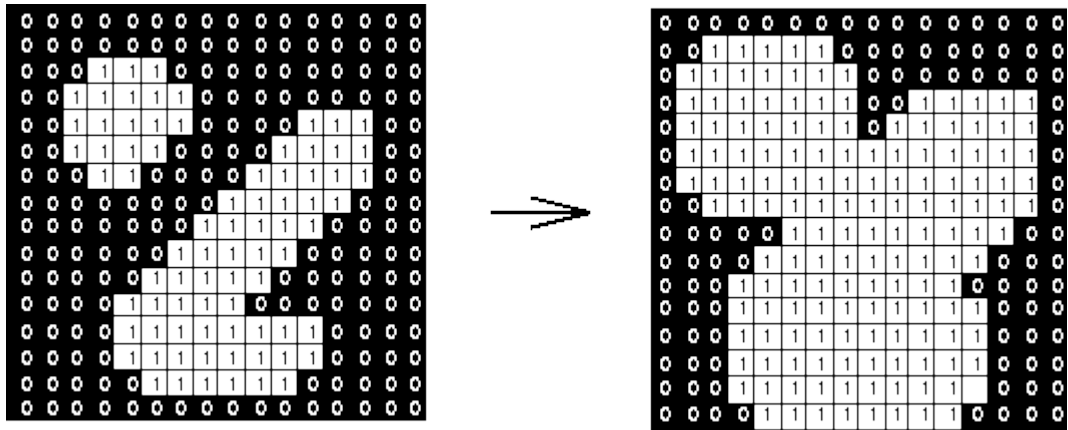
Figure 20: Effect of dilation using a 3×3 square structuring element. [30]

6. Practical part

Based on literature research, following experimental setup for Scratch Wound Healing Assay realization in microfluidics was proposed:

(1) Use microfluidic device Ibidi µ-Slide III 3in1 as 3D biomimetic environment. Microfluidic device Ibidi µ-Slide III 3in1 with two inlet microchannels and one outlet has design similar to PDMS-fabricated microfluidics, which was used in previous research for Scratch Wound Healing Assay. According to the product technical datasheet provided by manufacturer, Ibidi µ-Slide III 3in1 model is suitable for fluidic assays and compatible with pump. To analyze cells under microscope no special preparations are necessary. Cells can be observed directly in the µ-Slide III 3in1 on an inverted microscope. Transparency of model guarantee compatibility with laser-scanning confocal microscope. To ensure laminar flow and establish appropriate speed of fluid flow additional experiments were done. Calculation of shear stress applied by walls of microfluidic device was performed in order to compare with physiological value.

(2) Use Calcein AM and/or CellTracker™ Green CMFDA to label cultured cells in microfluidic device in order to perform image acquisition in fluorescent mode. As cell migration during wound healing can exceed 24 hours, it is crucial to insure, that cell labeling will last during that time. Cell labeling intensity was experimentally confirmed.

(3) Use trypsin flow to deliver scratch on cell monolayer. Due to closed geometry of Ibidi µ-Slide III 3in, it is impossible to create physical scratch, alternatively chemical scratch can be performed. To ensure laminar flow of trypsin and choose which inlet provides the most stable flow, additional experiments were performed.

(4) After 5 minutes of cells being exposed to trypsin, use laminar flow of PBS and medium solution to eliminate damaging impact of trypsin. Previous literature has shown that an often-reported problem associated with conventional Scratch Wound Healing Assay is the accumulation of cells across the edge of the scratch. In order to overcome this shortcoming in this study scratch was flashed with PBS and medium solution. [31]

(5) Perfuse cultured cells with 500 µl of fresh medium, as diffusion of nutrients and waste is limited when microchannels are not constantly perfused, and therefore cell migration can be impacted. [19]

(6) Take images of wound healing at timepoints 0 hours, 24 hours to observe wound closure.

(7) Use laser-scanning confocal microscope Leica TCS SP8 X, objective x10 for image acquisition.

(8) Analyze cell migration rate as closure of the wound over the time. Use MATLAB computing environment to perform image processing.

Following laboratorian equipment was used:

- Laminar flow extractor hood (BioAir)
- Incubator (Memmert)
- Centrifuge (BioTech)
- Laser-scanning confocal microscope Leica TCS SP8 X
- Inverted microscope Olympus IX-71
- Laboratory peristaltic pump Dynamax (Rainin) ×2

6.1 Microfluidic device Ibidi μ-Slide III 3in1

Ibidi μ-Slide III 3in1 is microfluidic device designed for microscopic analysis of fixed or living cells (Fig.21). It is made from the high optical quality material to enable fluorescence experiments with uncompromised resolution and choice of wavelength. Microfluidic device design allows generating fluid stable concentration profiles in the main channel for e.g. chemotaxis, cell migration experiments. [32]
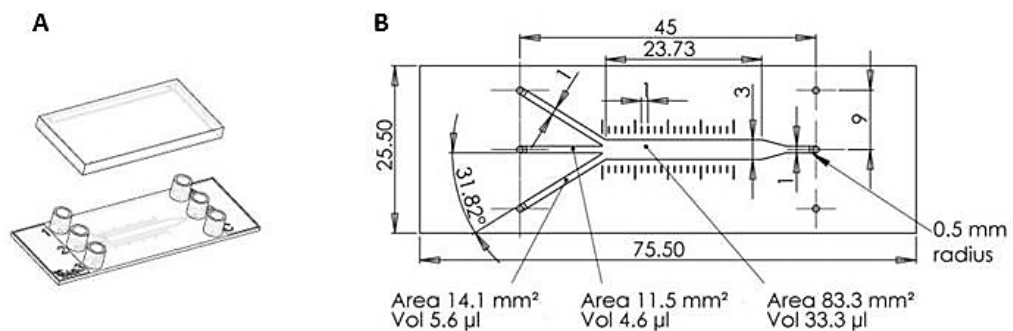
Figure 21: A) μ-Slide III 3in1. B) Microfluidic device geometry. [32]

Each of three reservoirs has volume of 500 μl, height of microchannel is 0.4 mm, width of microchannel is 3 mm. Total growth area for cells is 1.23 cm^2. Distance between the scale bars is 1 mm. Described properties constitute a favorable 3D biomimetic microenvironment for Scratch Wound Healing Assay.

6.2 Preparation of Ibidi μ-Slide III 3in1

Prior to cell seeding, microfluidic device Ibidi μ-Slide III 3in1 was covered with 60 μl partially purified fibronectin (Sigma-Aldrich, MI, USA) to promote cell adhesion. To prepare optimal conditions for attachment coated microfluidic device was incubated at 37 °C and 5 % CO$_2$ for 1 hours. After that fibronectin solution was removed and model was rinsed carefully

with PBS. According to the cell seeding protocol provided by the manufacturer, the day before seeding cells, device was filled with the cell medium and placed into the incubator for equilibration to prevent air bubbles formation over the incubation time. After culture medium solution was replaced with cell suspension solution. [32]

6.3   Cell culture in microfluidic device

According to cell seeding protocol provided by Ibidi μ-Slide III 3in1 manufacturer it was suggested to use cells with density from 3×10^5 to 7×10^5 viable cells per ml. When cell suspension with favorable density was prepared, input microfluidic channel was filled with 60 μl of cell suspension. After cells attached to the bottom, each reservoir was filled with 60 μl cell medium and incubated at 37 °C and 5 % CO_2.

Cell suspension was prepared according to cell subculture protocol. From prepared flask with confluent cell layer was removed medium and cells were rinsed with Trypsin – EDTA (0.5%). Cell detachment was encouraged by incubating at 37 °C and 5 % CO_2 for 3 minutes. After detachment, 5 ml of medium was added to neutralize the trypsin, then, to prepare suspension cells where centrifuged. After centrifugation supernatant was carefully discared, and replaced with 1 ml of medium, then mixed using pipet to create cell suspension. During cell subculture, DMEM medium formulated with the addition of 10 % FBS was used for 3T3 cells culturing, EGM-2 medium for HUVECs line, and Nutrient Mixture F-12 Ham for CHO cell line. [8], [9], [10], [32]

6.4   Cell labeling with fluorescent dues

Cells were labeled with the fluorescent dues in the day of culturing in the microfluidic device, once they adhere.

Following the labeling protocol provided by Calcein AM manufacturer, medium supernate was carefully discared from the microfluidic device and replaced with the 60 μl medim mixed with 0.1 μl Calcein AM solution. Microfluidic device was incubated at 37° C under 5 % CO_2 for 10 minutes, then medium was replaced with the 60 μl of fresh medium. Fluorescence was recored on confocal microscope Leica TCS SP8 X using a 495 nm excitation filter and a 505-55 nm emission filter. [33]

For labeling via CellTracker™ Green CMFDA, according to the protocol staining solution was prepared with 1:1000 dilution. Medium supernate was carefully discared from the microfluidic device and replaced with the 60 μl serum-free medim mixed with 0.06 μl CellTracker™ Green CMFDA staining solution. Microfluidic device was incubated at 37° C

under 5 % CO_2 for 30 minutes, then medium was replaced with 60 μl of fresh medium. Fluorescence was recored on confocal microscope Leica TCS SP8 X using a 492 nm excitation filter and a 505-555 nm emission filter. [34]

In oder to examine stability and persistence of cell labeling via fluorescent due within the 24 hours of wound healing process, cell labeling tests were performed. Microfluidic device with confluent cultured cell monolayer was labeled with Calcein AM according to the labeling protocol provided by the manufacturer. After labeling, images of cell sample were obtained with the confocal microscope Leica TCS SP8 X. During the experiment, microfluidic device Ibidi μ-Slide III 3in1 was taken out of the incubator at timepoints $t_1 = 0$ h, $t_2 = 24$ h, and placed under ×10 objective, where images were taken. At each of timepoints image intensity of the same field was compared. (Fig.22)
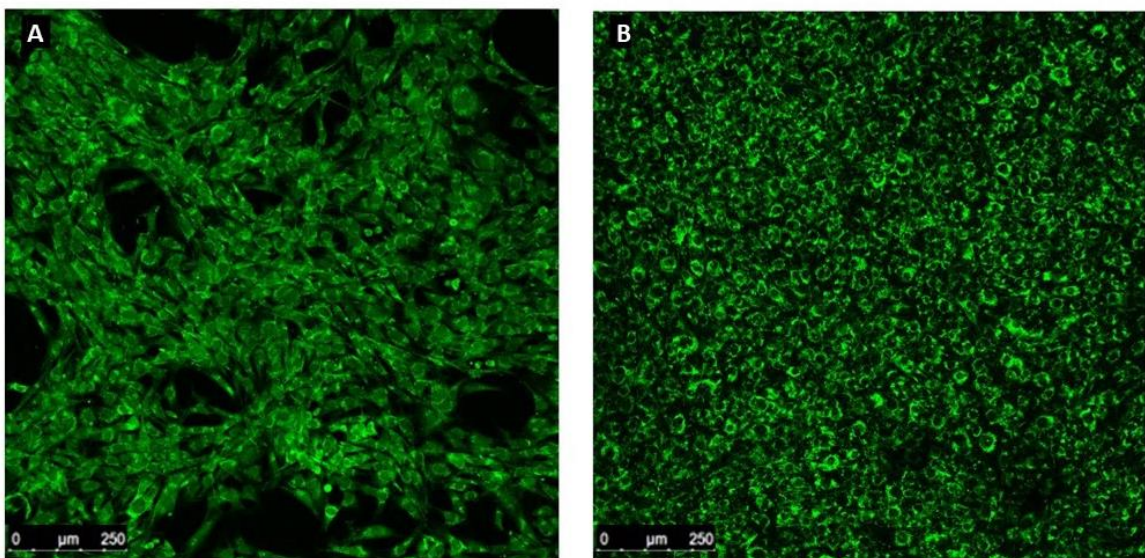
Figure 22: Cell labeling test. A: 3T3 cells labeled with fluorescent due Calcein AM in microfuidic device Ibidi μ-Slide III 3in1. An image field taken at t=0 h. B: 3T3 cells labeled with fluorescent due Calcein AM in microfuidic device Ibidi μ-Slide III 3in1. An image field taken at t=24 h. Scale bars 250 μm.

As it was observed from the experiment fluorescent due maintains persistent color intensity when used for labeling cells in microfluidic device. It also appears, that over 24 hours of incubation, 3T3 cells overgrew, what caused to the change of cells shape. This finding suggests, that use of fluorescent dues suit Scratch Wound Healing Assay realization in microfluidic device. It was also concluded, that time for observing cell activity in microfluidic device Ibidi μ-Slide III 3in1, preferably should not exceed 24 hours, otherwise cells behavior might be affected by limited access to the living media, with overgrowing cell population. For further cell labeling fluorescent due Calcein AM was used, as it showed successful results during testing – labeling persistence without damaging cell integrity over the time of 24 hours.

6.5 Formation of laminar flow in microchannels

Laminar flow (or streamline flow) is a condition in fluid dynamics, which occurs when there is no turbulence between two or more fluid flows in parallel layers (Fig. 23). [20]
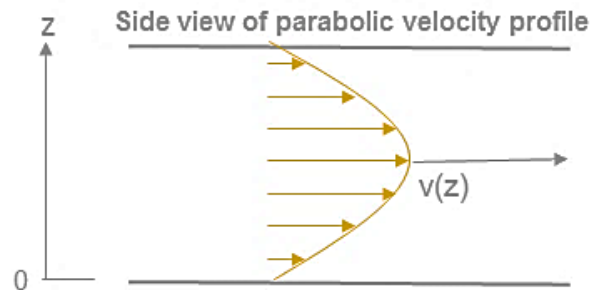
Figure 23: Velocity distribution created by a laminar flow. [35]

Testing of laminar flow formation in microfluidic device Ibidi μ-Slide III 3in1 was performed as described below. Inlet B was used as an outflow, inlet 1 was connected to the reservoir with pink-colored water, which was injected via pump, inlet 2 was tightly covered, and, inlet 3 was connected to the reservoir with discolored water (Fig.24). Two peristatic pumps were used. Through the testing of different fluid flow rates, the most stable laminar flow condition was observed with under the following conditions: first pump was connected to outflow inlet B with a speed at 0.25 ml/min, pulling out fluid from the microfluidic device, while second pump was connected to inlet 1 through the reservoir with the pink-colored water at the same fluid speed of 0.25 ml/min, thus delivering the fluid into microfluidic device. While first pump was creating pressure inside of the microchannel, second pump was loading the fluid, therefore resulting speed for fluid (pink-colored water) delivered through inlet 1 was calculated as the sum of the speeds $0.25 + 0.25 = 0.5$ ml/min; and resulting speed for fluid passively delivered through inlet 3 (colorless water) was 0.25 ml/min, as it was pulled out by the pump connected to outlet B.
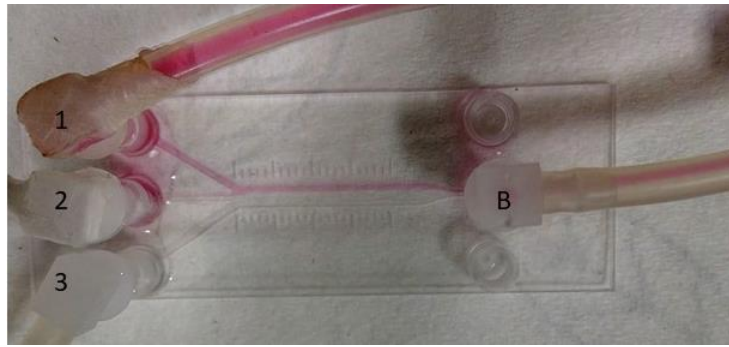
Figure 24: Testing of laminar flow conditions in Ibidi μ-Slide III 3in1. Inlet 1 – reservoir with colored water loaded by a pump, inlet 2 – covered, inlet 3 – colorless water, outlet B – trash disposal, connected to the pump, pulling out fluids from microfluidic device

6.6   Shear stress calculations for Ibidi μ-Slide III 3in1

It was described in previous literature that cell behavior is impacted by applied shear stress. Cells sense mechanical forces, what leads to mechanotransduction into biological responses. Impact varies in accordance to the cell line and includes such effects as change of morphology, proliferation and cell dissociation.

In conventional cell migration assays cells are not exposed to the mechanical forces including shear stress due to the sample geometry, which is a huge limitation of 2D cell cultures experiments. In contrast, microfluidics device design can provide a 3D biomimetic microenvironment which enables application of the shear stress. Therefore, the use of microfluidics device is a viable alternative to conventional in vitro techniques of scratch wound healing assy. Shear stress is a frictional force of a fluid acting on the cell layer on the wall. Shear stress, viscosity and shear rate are related by the following formula:

$$\tau = \eta \cdot \gamma \qquad (3)$$

Where τ is a shear stress, measured in Pa, η is dynamical viscosity of the fluid in $Pa \cdot s$, and γ is a shear rate in s^{-1}. The shear rate describes the velocity profile of the perfused fluid, while dynamic viscosity is a measure of fluid's internal resistance. Dynamic (absolute) viscosity is the tangential force per unit area required to move one horizontal plane with respect to another plane, when maintaining a unit distance apart in the fluid (Fig. 25).
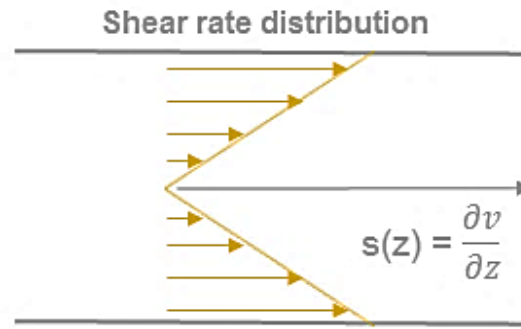
Figure 25: Shear rate distribution created by a laminar flow, where s(z) is the velocity gradient or shear rate (s^{-1}). [35]

To calculate shear stress for in main microfluidic channel of Ibidi μ-Slide III 3in1 (Fig.26), following equation provided by manufacturer was used:

$$\tau = \eta \cdot 227.4 \cdot \Phi \qquad (4)$$

where Φ is fluid flow measured in ml/s. [35]
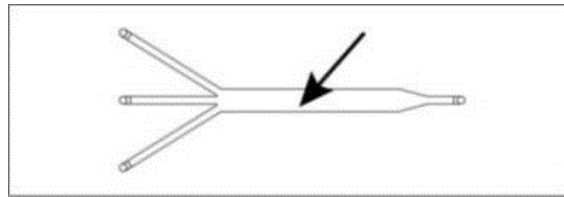
Figure 26: Ibidi μ-Slide III 3in1, 3 mm microchannel. [35]

Solution injected to the microfluidic device was either trypsin or medium, in accordance with the stage of the experiment. Dynamic viscosity η of both fluids was provided by manufacturer in datasheet. Table 1 demonstrates shear stress values in 3 mm microchannels during the application of trypsin and medium solutions. [35]

Fluid	Dynamic viscosity η, [$Pa \cdot s$]	Fluid low Φ, [ml/s]	Shear stress τ in 3 mm microchannel, [Pa]
Medium	0.00078	0.004	0.0014
Trypsin	0.00105	0.008	0.0019

Table 1: Shear stress values for trypsin and medium solutions in Ibidi μ-Slide III 3in1 microchannels.

The calculated shear stresses applied to the cell monolayer caused by the fluid flow belong to range from 0.0014 to 0.0019 Pa, this range lies within physiological values, since overall shear stress in circulation varies from 0.01-1.0 Pa in microvasculature, to above 3.0 Pa in large blood vessels, e.g. aorta. Therefore, shear pressure applied by the microfluidic device walls does not damage cell integrity.

It was observed that the width of the trypsin flow was slightly smaller near the outflow microchannel due to higher velocity and parabolic flow-rate distribution (Fig.27).
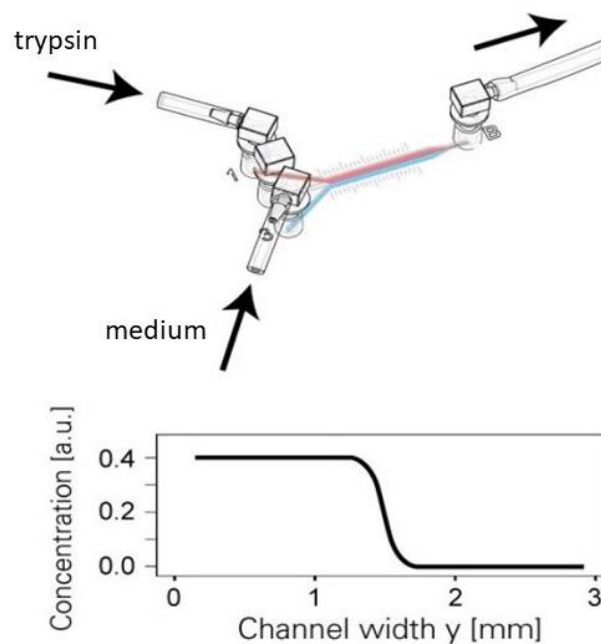
Figure 27: Cliff-shaped gradient. Gradient steepness of fluid in Ibidi μ-Slide III 3in1 microfluidic device. Inlet 1 - trypsin, inlet 2 - covered, inlet 3 – medium, outlet B – trash disposal. [32]

6.7 Chemical cell exclusion via trypsin

Physical scratch of the cell monolayer may result in cell damage near the wound edges and therefore affect cell migration process. Previous studies have shown that application of the laminar flow of trypsin solution in microfluidic channels enable controlled cell detachment of a portion of confluent cell monolayers. [20]

To assess chemical impact of trypsin on cell monolayer additional experiments of conventional Scratch Wound Healing Assay were performed. In this experiment 3T3 cells monolayer was cultured on the glass surface, which was kept in culture dish filled with DMEM

medium. Sample was placed in the incubator at 37 °C in 5 % CO_2 until cell monolayer reached conluence. Then, glass was removed from the culture dish, trypsin was slowly delivered to the middle of the glass through the low-volume syringe of 10 ml. Once wound was created glass was flashed with the PBS, placed to the dish with fresh DMEM medium and incubated at 37 °C in 5 % CO_2. Medium was replaced every 24 hours. Images of wound were taken after 24 and 42 hours of wound creation. It appeared that wound created under the chemical impact of trypsin healed completely within 24 hours. After 42 hours cell overgrowth on cell-covered region was observed (Fig. 28).
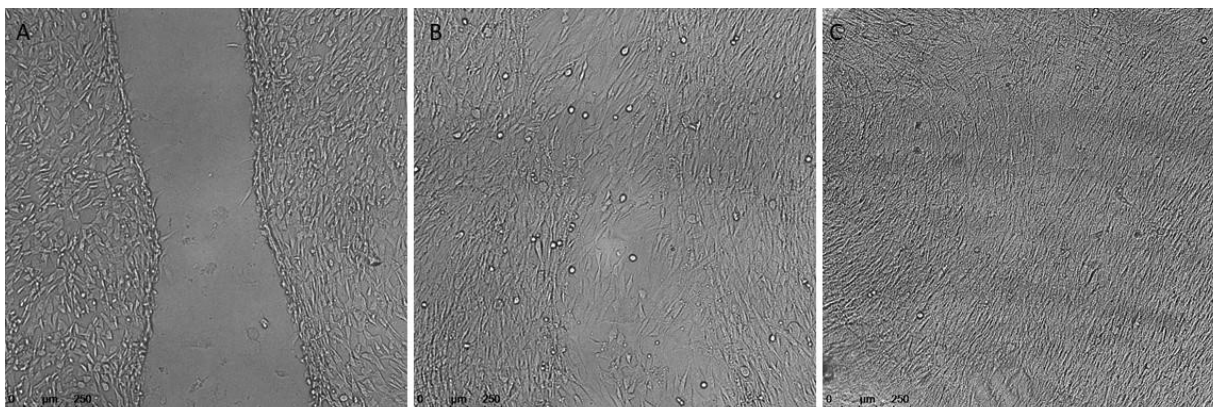
Figure 28: Chemical impact of trypsin on cell monolayer culture on tha glass. A: Creation of the wound. B: Wound closure after 24 hours. C: Overgrowth cell culture after 42 hours. Scale bars, 250 μm.

Given that closed-channel structure of Ibidi μ-Slide III 3in1 microfluidic device does not allow to deliver physical scratch of the cell monolayer or deliver trypsin directly to the cell layer, cell exclusion was generated by introducing laminar trypsin flow to the one out of four microchannels. Experiment was performed in two installments. At the first place, reservoir filled with trypsin was connected to the inlet 1 of Ibidi μ-Slide III 3in1 through the peristatic pump. Fluid speed was set to 0.25 ml/min. Inlet 2 was tightly closed with silicone cover. Inlet 3 was connected to the reservoir with medium, however medium was pumped passively, without using pump. Second peristatic pump was connected to outlet B, thus creating negative pressure, with the fluid flow speed set at 0.25 ml/min, and pulling fluid out of the microfluidic device to the empty reservoir serving as trash-disposal (Fig. 29). Microfluidic device contained cultured cell monolayer. After 5 minutes, when trypsin at the amount of 2.5 ml went through the cell monolayer, trypsin supply was stopped, and experimental setup was changed.
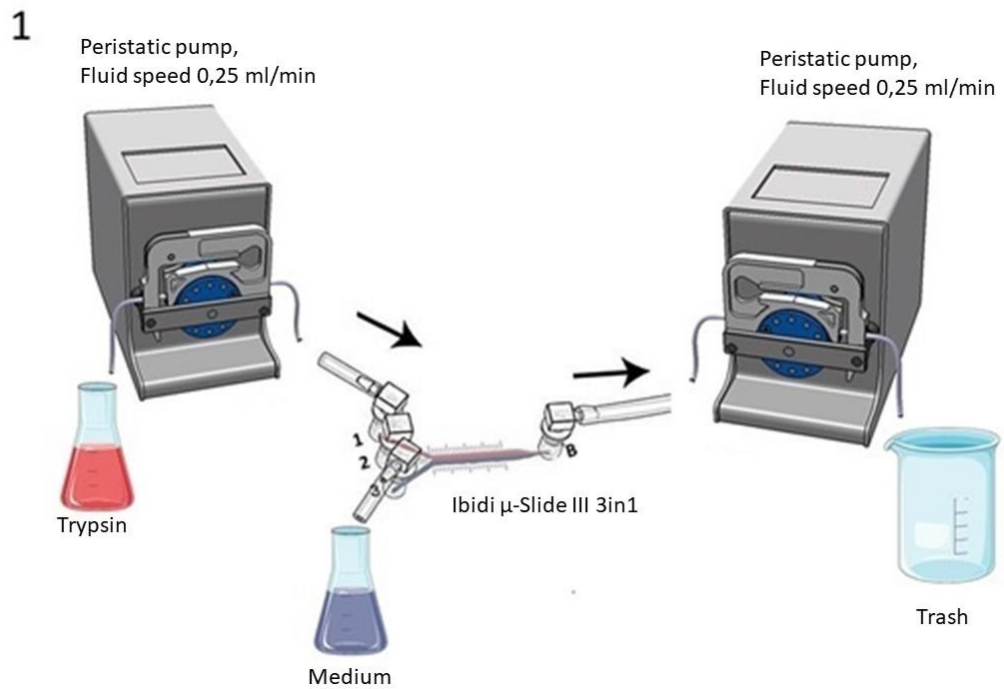
Figure 29: Schematic illustration of the installment 1: Peristatic pump Dynamax (Rainin) ×2, fluid speed set to 0,25 ml/min; reservoir with trypsin and medium, empty reservoir; Ibidi μ-Slide III 3in1: inlet 1 connected to reservoir with trypsin through the pump, inlet 2 covered, inlet 3 passively connected to reservoir with medium, outlet B connected to the empty reservoir through the pump.

Inlet 1 was filled with 500 μl of PBS. Reservoir with trypsin was replaced with reservoir with the medium, then fluid supply at the same speed was resumed. (Fig. 30). Medium was delivered for 5 minutes in total amount of 3.75 ml (2.5 ml delivered through inlet 1 via pump and 1.25 ml delivered passively through inlet 3), then supply was stopped, microfluidic device was covered and incubated at 37 °C in 5 % CO_2. Both installments were performed under real-time image acquisition using laser-scanning confocal microscope Leica TCS SP8 X, objective x10.

Every 24 hours 500 μl of fresh serum-free medium were injected to the inlet 2, while simultaneously 500 μl of fluid were removed from outlet B.
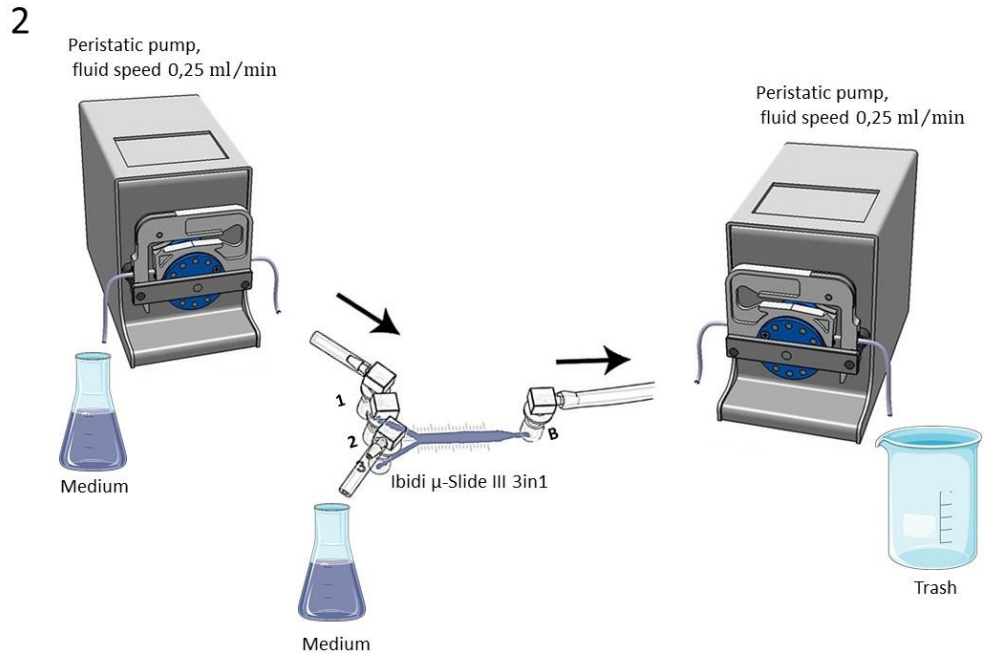
Figure 30: Schematic illustration of the installment 2: Peristatic pump Dynamax (Rainin) ×2, fluid speed set to 0,25 ml/min; reservoir with medium ×2, empty reservoir; Ibidi µ-Slide III 3in1: inlet 1 connected to reservoir with medium through the pump, inlet 2 covered, inlet 3 passively connected to reservoir with medium, outlet B connected to the empty reservoir through the pump.

It appeared that cells which covered region exposed to the trypsin flow were detached from the surface and flushed, whereas cells which were not in the direct contact with the trypsin flow remained attached. (Fig. 31). Cells exposed to the trypsin flow tend to change its shape during 2-3 minutes of trypsin application. It was observed that majority of cells exposed to the trypsin flow would be flushed after 5 minutes of trypsin application.
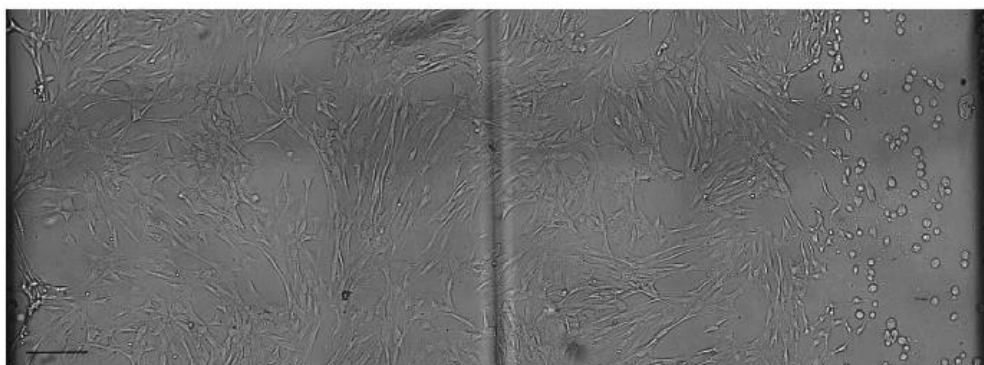
Figure 31: 3T3 cell monolayer cultured in microfluidic device Ibidi µ-Slide III 3in1 under trypsin flow (right side, round-shaped cells). Scale bar 250 µm.

Cell dissociation using trypsin (trypsinization) is performed by breaking down cell proteins (amino acids on their C-terminus) which enable the cells to adhere. When trypsinization

procedure is complete, affected cells appear round shaped and carried away with the flow. As a result, cell integrity is not being disrupted. [36]

Effect of wound healing was examined every 24 hours. For this purpose, image acquisition was performed.

6.8 Image processing algorithm

A common method to analyze the process of cell migration is to use a bright-field images of the scratch at predetermined time-points with following analysis of the gap closure. During the experiment, microfluidic device was taken out of the incubator at timepoints 0 hour and 24 hour and placed under a Leica TCS SP8 X with a ×10 objective, where pictures of fixed positions were taken. The Scratch Wound Healing Assay is utilized to quantify wound closure over the time. Quantitative analysis of obtained images was provided using a custom-made algorithm in MATLAB software (R2018b 64-bit, MathWorks®, USA). Wound areas (WA) measurements from individual images was used to calculate migration rates. WA was defined as the ratio of the cell-free area relative to the total image size.

$$WA = \frac{\text{Number of White Pixels}}{\text{Total Image Area}} \tag{5}$$

In order to obtain reliable results, WA was quantified across multiple frames of the image from the same cell sample for every timepoint to determine whether wound area changes over the time are statistically significant. Image processing algorithm is described on the scheme below (Fig. 32). Step by step image segmentation for edge detection is illustrated on Fig.33.
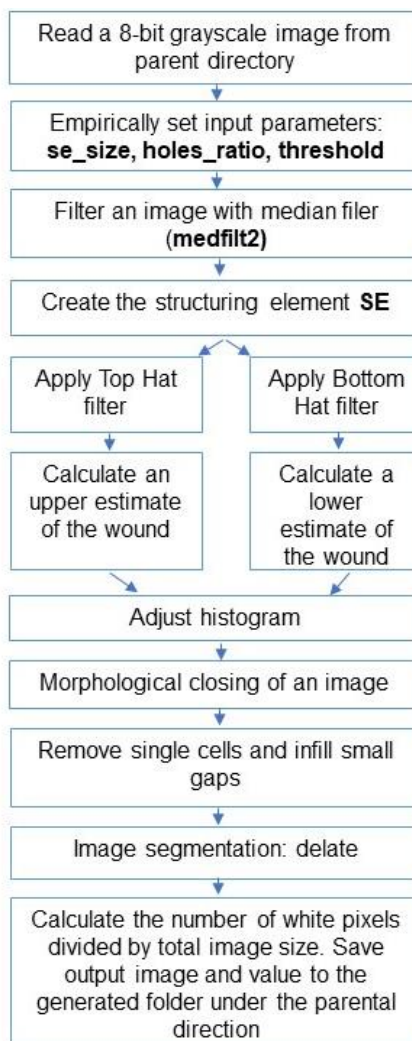
Figure 32: Image processing algorithm flow-chart.
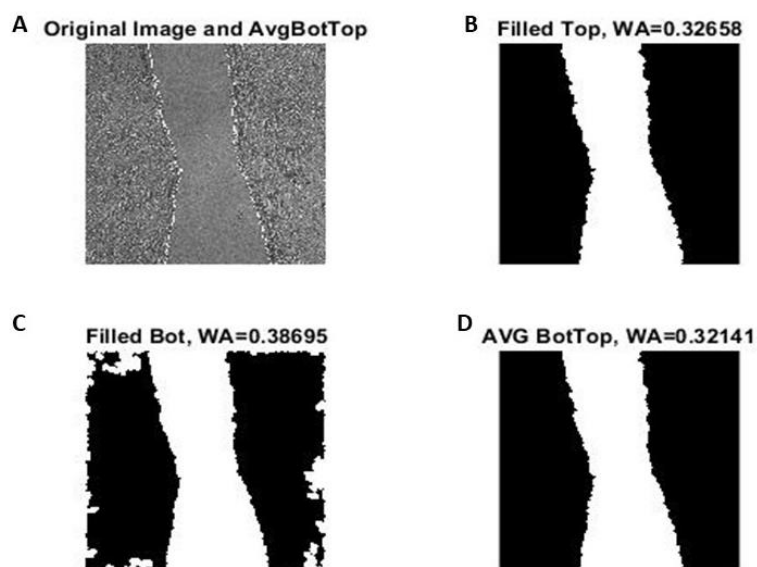
Figure 33: Image segmentations steps. A: Original image with an edge. B: Top-hat filtering. C: Bottom-hat filtering. D: Edge detection.

Input grayscale image was filtered with a median filter to reduce random noise and slightly smooth edges. Then edges were filtered with a Top-hat and Bottom-hat filters to calculate an upper and a lower estimate of the wound and adjust histogram. Segmentation of an image was performed with se_size, holes_ratio, and threshold input parameters, with were found empirically. Output WA was calculated as the number of white pixels divided by total image size.

6.9 Results

Proposed experimental setup for Scratch Wound Healing Assay in microfluidic device was realized for endothelial cell lines HUVEC and CHO, and fibroblast 3T3 cells. Cell samples were prepared accordingly to culture protocols using seeding instructions from Ibidi μ-Slide III 3in1 microfluidic device manufacturer described above.

Results of HUVECs culture in microfluidic device before creation of wound via trypsin are presented below. Figure 34.A shows that cells are uniformly distributed on the surface inside of the device, however with the closer look (Fig. 34.B), it appears that cells do not show strong cell to cell connections, and mostly presented as a single cells or a small groups, rather than confluent cell monolayer. In such a case, trypsin was not applied, cell sample was allowed to grow and reach required confluency. However, cells showed the same condition after additional 24 and 48 hours of incubation. Low cell adherence, round shape and evidence of damaged cell structures were observed. Experiment was repeated with increased cell seeding density, however HUVECs have not shown desired cell confluence to undergo the next trypsinization step of the experiment.
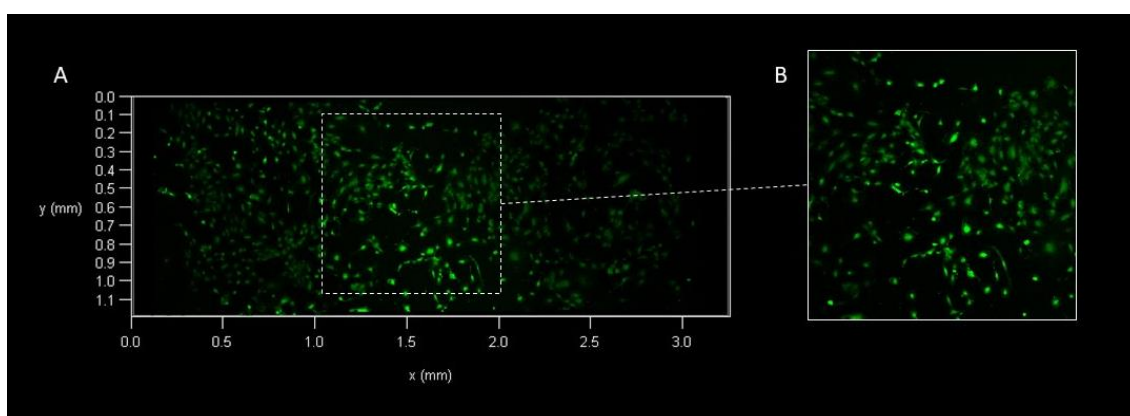
Figure 34: HUVECs labeled via Calcein AM, cultured in microfluidic device Ibidi μ-Slide III 3in1 before application of trypsin. A) Sample surface cell coverage, width view. B) Center filed zoomed in 1,5 times.

In order to understand this outcome, we though to repeat experiment using another endothelial cell line with the similar cell morphology – CHO cells. Seeding cell density was

chosen following seeding instructions for Ibidi μ-Slide III 3in 1 microfluidic device. CHO cell distribution is shown on Fig.35. With the similar to HUVECs distribution, cells were able to adhere and elaborate polygonal shape typical for epithelial cell type morphology. At the same time, as it can be noticed on Fig. 35.B and Fig.35.C, there were gaps presented between cells. Since cell confluence was achieved for CHO cells, trypsin was applied to cell monolayer using experimental instalment described above. Fig.36 was taken right after application of trypsin. It shows cell coverage decrease across the entire area of cell sample, even though trypsin flow was only targeted to the left side of the microfluidic device. It was expected that wound will appear on the left side and would not cover more than 50% of the area. With the majority of cell population flushed with the trypsin flow during the wound creation, CHO cell sample did not show wound healing after 24 and 48 hours of incubation.
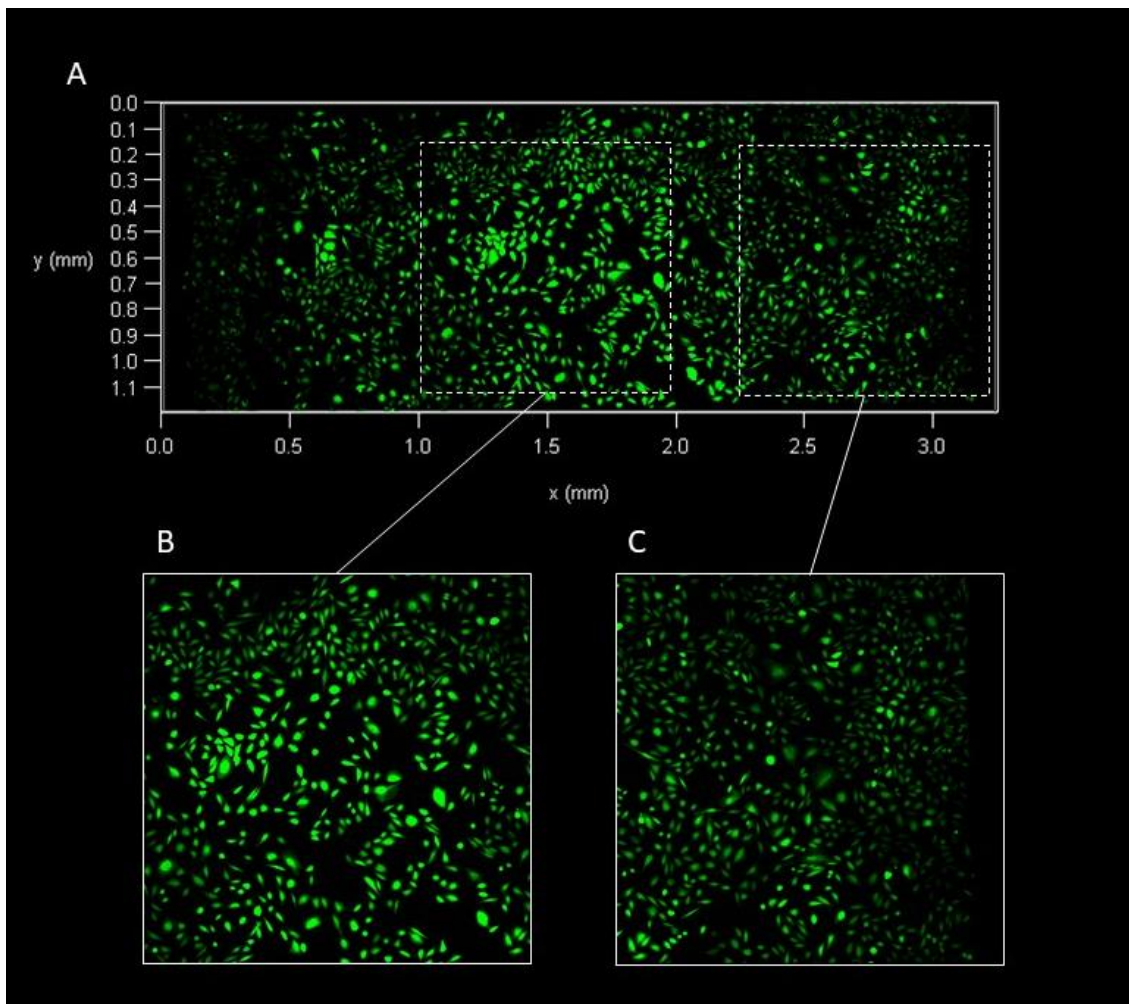
Figure 35: CHO cells labeled via Calcein AM, cultured in microfluidic device Ibidi μ-Slide III 3in1. A) Sample surface cell coverage, width view. B) Center filed zoomed in 1,5. C) Edge field zoomed in 1,5 times.
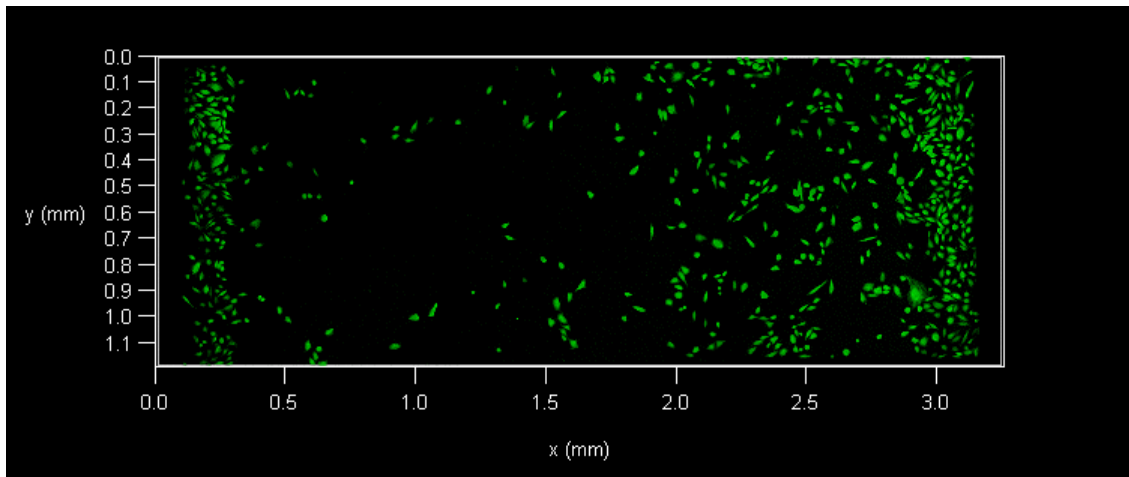
Figure 36: CHO cells labeled via Calcein AM in microfluidic device Ibidi µ-Slide III 3in1, image was taken right after the application of trypsin.

In order to compare these findings to different cell morphology type, as the next step, we repeat this experiment for fibroblasts, 3T3 cell line.

As it can be observed on Fig.37, adhered 3T3 cells reached confluence and create tighter cell to cell connections. Gaps were still presented, however they tend not to be connected with each other. 3T3 cell sample underwent trypsinization step. Wound of expected size was created on the left side of the field. Adjacent cells were not damaged by chemical impact of trypsin. Wound healing over the time was observed.
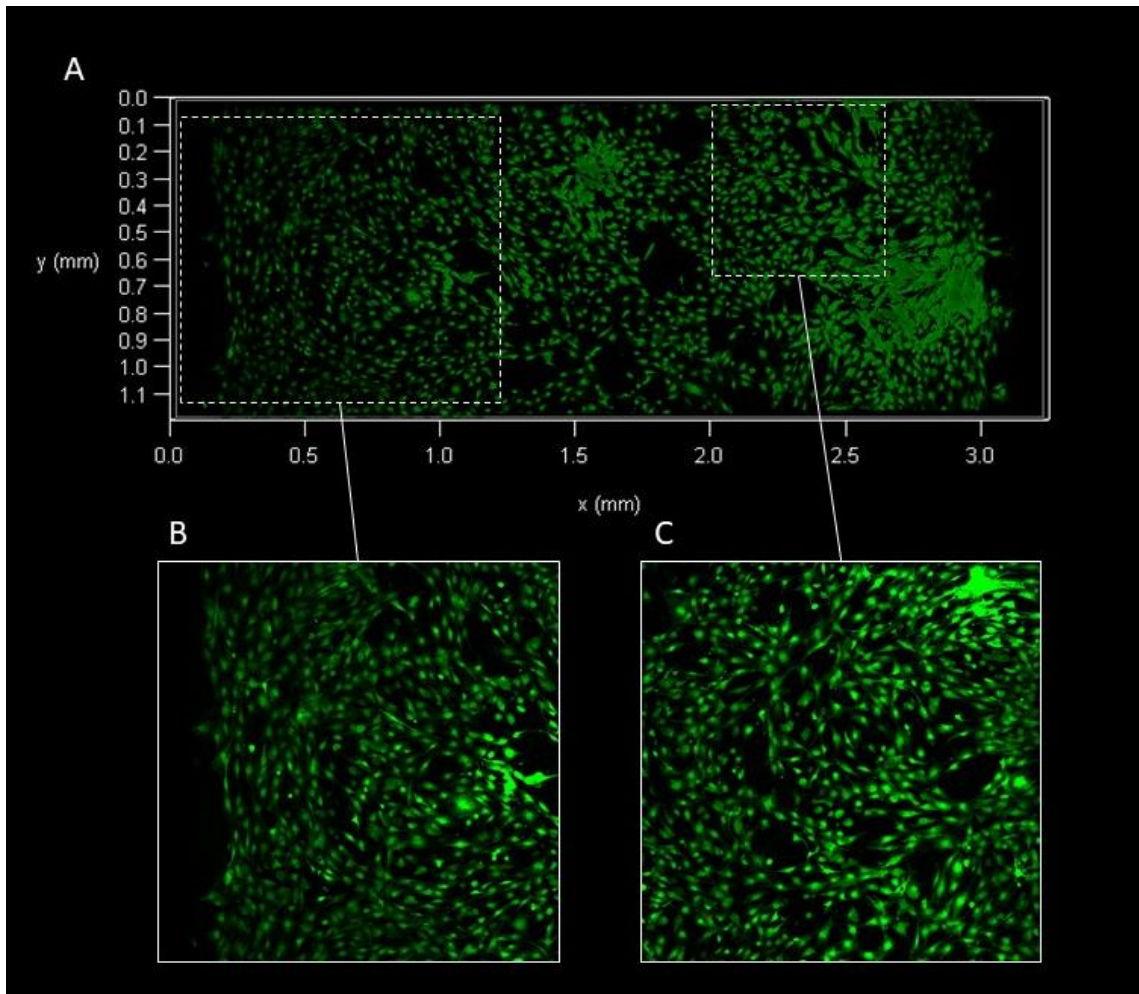
Figure 37: 3T3 cells labeled via Calcein AM in microfluidic device Ibidi μ-Slide III 3in1, image was taken before the application of trypsin. A) Sample surface cell coverage, width view. B) Edge field zoomed in 1,5. C) Field zoomed in 2,3 times.

Following parameters of wound closure were analyzed:

- Wound area (WA): inversed cell covered area [%], [mm].
- Speed of wound closure [mm/hour].
- Linear approximation of wound closure [%/hour], [mm/hour].

In total 8 randomly chosen fields of the same size (512×512), where analyzed at timepoints t_1 – after creation of wound, t_2 – after 24 hours of incubation. For 3T3 cells cultured in microfluidic device Ibidi μ-Slide III 3in1, calculated WA on the images obtained at t_1 right after the trypsinization, have mean of 23.82 ± 4.0 % or 0.2382 ± 0.04 mm, of total field area. After 24 hours of incubation, at t_2 WA mean decreased to 17.99 ± 4.0 % or 0.1799 ± 0.04 mm, of total field area. Speed of wound closure over the 24-hour period was 2.4 μm/h. Linear approximation of wound closure speed is shown on the Fig.38.
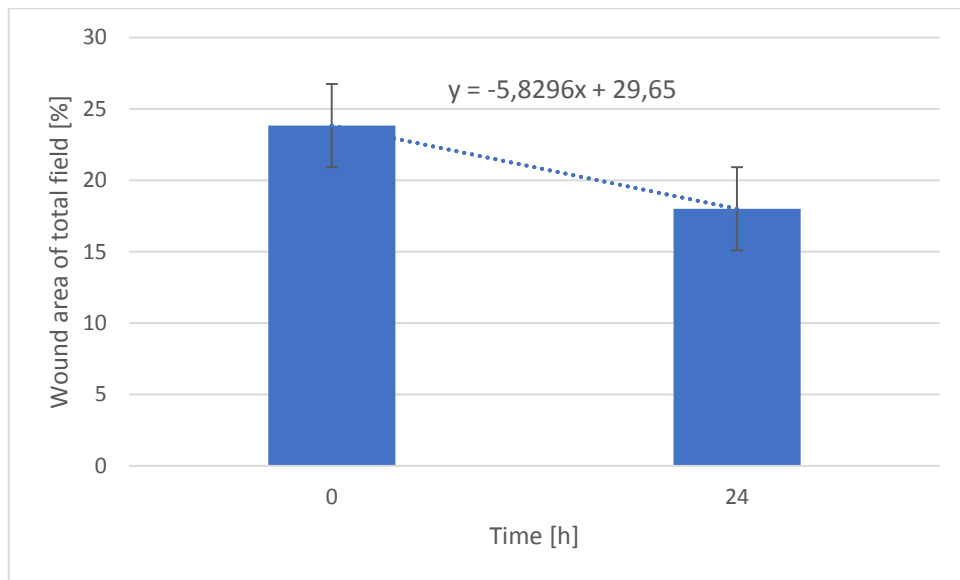
Figure 38: 3T3 cells in 3D microfluidic device. Wound closure over the 24-hour period.

In order to assess efficacy of custom-made algorithm for wound closure analysis, results were compared with values obtained from automated image processing software. For this purpose, WAs of the same fields were calculated in an open source image processing software Fiji ImageJ, manually defining the WA as the region of interest (Fig. 39).
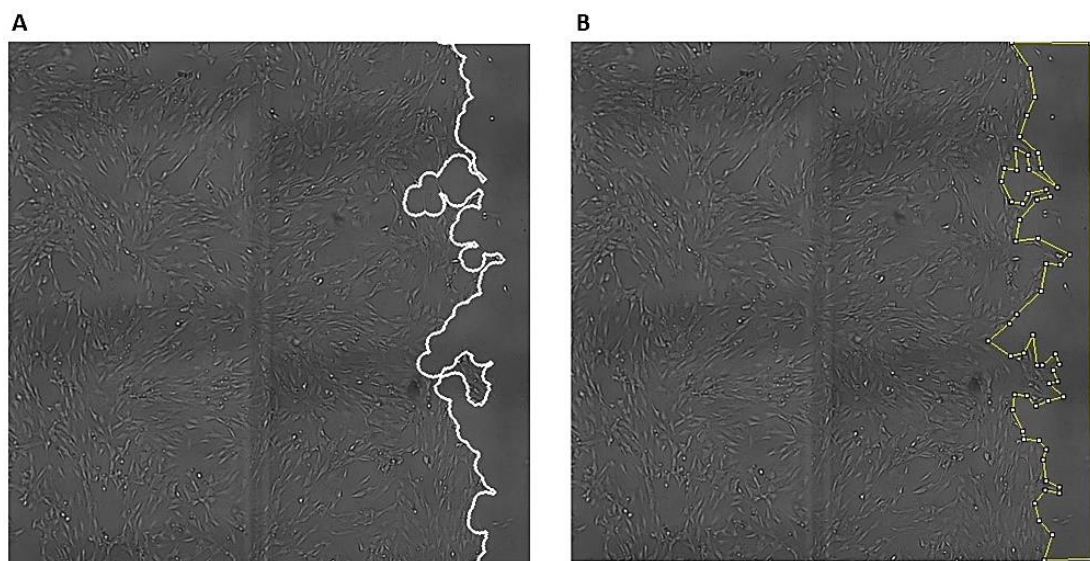
Figure 39: Detection of WA area. A) WA was detected and calculated using custom-made algorithm. B) WA was manually defined in image processing software Fiji ImageJ.

In total, 16 image fields were analyzed using different methods, 8 fields from t_1 and t_2. The two-tailed test was used for comparison. There was no significant difference between measurements obtained from a custom-made algorithm and image processing software. At significance level of 0.05, p-value equals 0.9342 and 0.6982, respectively for t_1 and t_2 (Tab. 2).

	Day 1: Wound creation		Day 2: Wound closure	
Image field	WA [mm]		WA [mm]	
	Algorithm	Fiji ImageJ	Algorithm	Fiji ImageJ
1	0.3156	0.2923	0.2775	0.2692
2	0.2133	0.2236	0.1402	0.114
3	0.2842	0.2622	0.1674	0.1475
4	0.2159	0.2399	0.1736	0.175
5	0.2170	0.2192	0.1899	0.1786
6	0.1984	0.1976	0.1863	0.186
7	0.2193	0.2153	0.1559	0.1498
8	0.2415	0.2437	0.1482	0.1488
Mean	0.238207	0.236725	0.179911	0.171112
SD	0.040744	0.02991768	0.043124	0.045803
The two-tailed P value	0.9342		0.6982	

Table 2: Comparison of WA calculated via custom-made algorithm and Fiji ImageJ algorithm processing software.

We thought to compare achieved results with wound closure outcomes using conventional 2D technique. For this purpose, we analyzed results obtained from trypsin chemical impact testing on cell monolayer, described above at 6.7. In total, 10 random fields were analyzed. 5 from an image taken after the trypsinization, and 5 from an image taken 24 hours after the incubation. Custom-made algorithm was used to calculate WA (Fig.40).
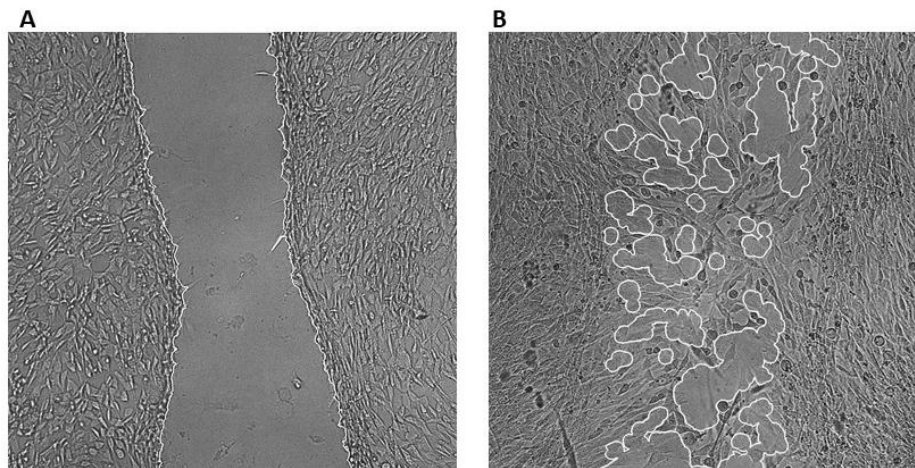
Figure 40: 3T3 cell line cultured on a glass. A) Wound creation. B) Wound closure after 24 hours

At t_1, right after the trypsinization, WA have mean of 53.78 ± 23.73 % or 0.5378 ± 0.2373 mm, of total field area. After 24 hours of incubation, at t_2, WA mean decreased to 39.08 ± 18.36 % or 0.3908 ± 0.1836 mm, of total field area. Speed of wound closure over the 24-hour period was 6.1 μm/h. Linear approximation of wound closure speed is shown on the Fig.41.
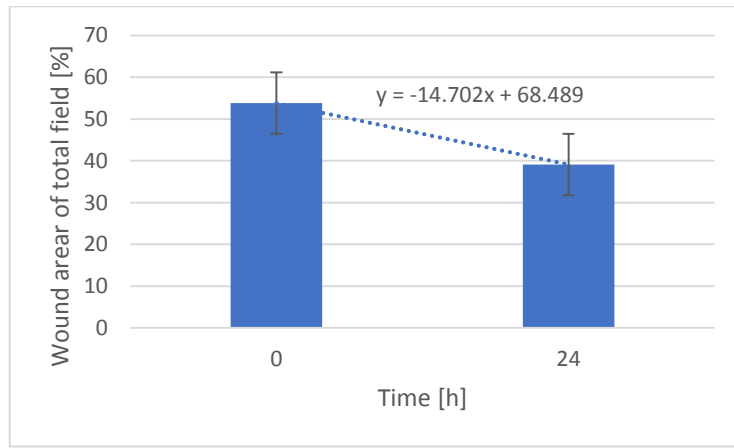
Figure 41: 3T3 cells culture on 2D environment. Wound closure over the 24-hour period.

7. Discussion

The goal of this thesis was to develop experimental setup Scratch Wound Healing Assay realization in microfluidic device using trypsin – EDTA for creation of cell delusion, and confocal microscope Leica TCS SP8 X for subsequent image acquisition; perform experiment with sufficient number of iterations, analyze wound closure with a custom-made algorithm written in MATLAB computing environment, and discuss achieved results.

Literature research was performed in order to develop experimental setup. Proposed conditions for experimental setup are listed in chapter 6. Every aspect of experimental setup for microfluidic realization of Scratch Wound Healing Assay was tested on a separate setting to assess effectivity and confirm that each of proposed conditions does not damage cell integrity and would not affect the total outcome. In total, proposed experimental setup was tested on two different types of cell morphology, on three different cell lines.

Microfluidic device Ibidi µ-Slide III 3in1 was chosen due to its suitable properties, however as to our knowledge, Scratch Wound Healing Assay was never performed using this microfluidic device, number of additional tests, such as ability of laminar flow creation and shear stress applied by the device walls, were performed to confirm device compatibility with the Scratch Wound Healing Assay.

Epithelial morphology type cell line HUVECs did not adhere enough to undergo trypsinization step of the experiment. There was observed network of gaps between the cell groups and poor cell to cell connections. Additionally, cells shape was damaged. This finding might be explained by either unsuitable conditions for cell growth inside of the microfluidic device or by initial inability of this cell population to grow. To understand this finding, another epithelial type morphology cell line - CHO cells, was tested. In this case, cells performed better and were able to adhere, as well as there was no notice of damage cell structures. CHO cells sample reached satisfactory condition to undergo trypsinization. However, with gaps presence, majority of cell population were flushed with trypsin flow, experiment was terminated, and did not undergo wound healing observation.

In this thesis it was observed, that behavior of epithelial morphology types – HUVECs and CHO cells, was not suitable for realization of Scratch Wound Healing Assay. This observation might be explained by the way how these cells migrate and grow. Whereas single-cell migration mechanism results in creation of the number filopodia and lamellipodia, and therefore allows to cover surface with a tight distribution of cell layer, collective cells migration

is guided by a leader cell (Fig.4), and thus less lamellipodia are created, what results in gaps presence between the cells. For realization of Scratch Wound Healing Assay in microfluidic device, presence of gaps may follow by chemical damage of cells over the entire surface of the cell monolayer. However, there is not enough evidence to prove this relation. Additional tests with different cell lines of epithelial morphology are required.

Fibroblast morphology is another type which was tested in practical part of this thesis. In contrast to epithelial-like cells, 3T3 fibroblasts showed satisfactory results and were able to undergo every step of experimental installment. Although, gaps were still observed, it did not cause a destruction cell layer integrity, as gaps were disconnected from each other, therefore, trypsin fluid was not able to spread among entire volume of the sample. This finding supports previous hypothesis that there might be connection between cell migration type and cell behavior in 3D system. More various cell lines should be tested to test this hypothesis.

A custom-made algorithm was written for the calculation of wound area. To analyze wound closure over the time. Wound area was calculated on images taken at two timepoints, $t_1 -$ is an image taken right after trypsinization was performed, and $t_2 -$ is an image taken after 24 hours of sample incubation at 37 °C in 5 % CO_2. At every timepoint 8 randomly chosen fields among the image were analyzed. Wound area was described as mean ± SD. Same fields were analyzed using widely used image-processing software Fiji ImageJ. There was no significant difference between wound areas calculated via custom-made algorithm and manual tool Fiji ImageJ. Therefore, it can be concluded that algorithm performed satisfactorily.

To gain a better understanding on how microfluidic device architecture affects cell behavior, 3T3 cells wound closure characteristics over the time cultured in microfluidic device and using trypsin for cell delusion was compared with 3T3 cells wound closure characteristic over the time cultured conventionally on a glass using trypsin for creation of cell delusion. It was observed, that wound created in microfluidic device had smaller dimensions and more regular, straight profile, while wound created on a glass was bigger. Wound areas were 23.82 ± 4.0 % 53.78 ± 23.73 % of total field size for cells cultured in microfluidic device and glass, respectively. In both cases wound area decreases within following 24 hours of incubation. After 24 hours wound areas were 17.99 ± 4.0 % and 39.08 ± 18.36 %. For both experiments linear approximation of wound closure speed was calculated. It appears that for cells cultured in microfluidic device linear approximation of speed was y = -5.8296x + 29.65, whereas for cell cultured on a glass in was y = -14.702x + 68.489. As we can see, speed of wound closure for cells cultured on a glass where higher 2.3 times. The same ratio is observed if compare wound

areas from both experiment settings at timepoint 1 and timepoint 2. This finding suggests, that there is a linear relation between wound closure speed and wound area.

Finally, we compared migration speeds for fibroblasts in 2D and 3D environment with findings of the previous research. Previous literature suggests that fibroblast migration speed is depended on experimental conditions. In a study where behavior of 3T3 cells migration rates were compared in 2D and 3D, it was suggested that migration rates are 18 μm/h and 29 μm/h, in 2D and 3D environments respectively. In this study migration rates were slower as 2.4 μm/h and 6.1 μm/h, for 2D and 3D models. This difference can be explained that in previous research chemical factors known for promotion of migration process were used. Additionally, geometry of 2D and 3D used is this thesis and previous research were different, hence not one-to-one, but only rough comparison can be performed.

Limitations of this thesis include limited number of microfluidic devices Ibidi μ-Slide III 3in1 used for practical part. For experiment iterations, every microfluidic device was sterilized and reused. There is no strict restriction regarding it, however manufacturer does not suggest multiple use of the device. Additionally, every subcultured cell line used for testing was originated from the same primary cell culture. We cannot know whether primary cell line was initially unsuitable for experimental purposes.

8. Conclusion

In this thesis, experimental setup for realization of Scratch Wound Healing Assay was proposed based on literature research. Three different cell lines were used for testing proposed experimental model. With the number of experiment iterations there was observed different behavior among the cell types. While proposed experiment was successfully realized with 3T3 fibroblasts, HUVECs and CHO cells did not complete experiment. For 3T3 cells wound closure was analyzed under two different experimental settings: (1) conventional Scratch Wound Healing Assay with use of trypsin for wound creation, and (2) microfluidic realization of Scratch Wound Healing Assay with use of trypsin for wound creation. Analysis of wound closure was performed using custom-made algorithm. Results obtained from custom-made algorithm were compared with results obtained using manual tool in Fiji ImageJ image-processing algorithm. There was no significant difference between results achieved. Results obtained from experimental setting (1) and (2) were compared. Linear relation between wound closure speed and wound area was observed in both experiments.

To conclude, developed experimental design of Scratch Wound Healing Assay using microfluidic device Ibidi μ-Slide III 3in1; showed reproducible and reliable technique for an assay realization in 3D biomimetic environment. This experimental setting enables advantage of precise control of the experimental conditions, excellent optical properties, and additionally application of shear stress and generating parallel flows.

References

[1] CELL CULTURE BASICS: Vanderbilt University [online]. [cit. 2019-05-02]. Dostupné z: https://www.vanderbilt.edu/viibre/CellCultureBasicsEU.pdf

[2] KAPAŁCZYŃSKA, Marta, Tomasz KOLENDA, Weronika PRZYBYŁA, Maria ZAJĄCZKOWSKA a TERESIAK. 2D and 3D cell cultures – a comparison of different types of cancer cell cultures. Archives of Medical Science. 2016, 9. DOI: 10.5114/aoms.2016.63743. ISSN 1734-1922. Dostupné také z: https://www.termedia.pl/doi/10.5114/aoms.2016.63743

[3] EDMONDSON, Rasheena, Jessica Jenkins BROGLIE, Audrey F. ADCOCK a Liju YANG. Three-Dimensional Cell Culture Systems and Their Applications in Drug Discovery and Cell-Based Biosensors. ASSAY and Drug Development Technologies. 2014, 12(4), 207-218. DOI: 10.1089/adt.2014.573. ISSN 1540-658X. Dostupné také z: http://www.liebertpub.com/doi/10.1089/adt.2014.573

[4] KOLEDOVA, Zuzana. 3D Cell Culture: An Introduction. 3D Cell Culture. New York, NY: Springer New York, 2017, 2017-06-21, , 1-11. Methods in Molecular Biology. DOI: 10.1007/978-1-4939-7021-6_1. ISBN 978-1-4939-7019-3. Dostupné také z: http://link.springer.com/10.1007/978-1-4939-7021-6_1

[5] Thermo Fisher Scientific: Technical Reference Library: Introduction to Cell Culture [online]. [cit. 2019-05-02]. Dostupné z: https://www.thermofisher.com/us/en/home/references/gibco-cell-culture-basics/introduction-to-cell-culture.html

[6] Fundamental Techniques in Cell Culture Laboratory Handbook – 2nd Edition. SigmaAldrich Co. 2001 [online]. [cit. 2019-05-02]. Dostupné z: http://www.bristol.ac.uk/safety/media/gn/ecacc-handbook-gn.pdf

[7] Sigma - Aldrich: Life Science. Cell Culture: Cell Culture Reagents [online]. [cit. 2019-05-02]. Dostupné z: https://www.sigmaaldrich.com/life-science/cell-culture/cell-culture-reagents.html

[8] NIH3T3 Cells: Subculture Protocol [online]. [cit. 2019-05-02]. Dostupné z: http://www.nih3t3.com/cell-culture-information/

[9] BAUDIN, Bruno, Arnaud BRUNEEL, Nelly BOSSELUT a Michel VAUBOURDOLLE. A protocol for isolation and culture of human umbilical vein endothelial cells [online]. [cit.

2019-05-02]. DOI: 10.1038/nprot.2007.54. ISBN 10.1038/nprot.2007.54. Dostupné z: http://www.nature.com/doifinder/10.1038/nprot.2007.54

[10] Creative Biolabs: Mammalian (non-human) Cell Lines CHO Cell Lines [online]. [cit. 2019-05-02]. Dostupné z: http://www.gmp-creativebiolabs.com/cho-cell-lines_65.htm

[11] LADOUX, Benoit a Alice NICOLAS. Physically based principles of cell adhesion mechanosensitivity in tissues: treaties and international agreements registered or filed and recorded with the Secretariat of the United Nations. Reports on Progress in Physics. 2012, 1986, 75(11). DOI: 10.1088/0034-4885/75/11/116601. ISSN 0034-4885. Dostupné také z: http://stacks.iop.org/0034-4885/75/i=11/a=116601?key=crossref.b044763aee934da5c40db28c4eff1ad1

[12] TERJUNG, Ronald, ed. Comprehensive Physiology: Cell Migration. 2012. DOI: 10.1002/cphy.c110012.

[13] MICHAELIS, U. Ruth. Mechanisms of endothelial cell migration: Cell Migration. Cellular and Molecular Life Sciences. 2014, 2012, 71(21), 4131-4148. DOI: 10.1007/s00018-014-1678-0. ISSN 1420-682X. Dostupné také z: http://link.springer.com/10.1007/s00018-014-1678-0

[14] JONKMAN, James E. N., Judith A. CATHCART, Feng XU, Miria E. BARTOLINI, Jennifer E. AMON, Katarzyna M. STEVENS a Pina COLARUSSO. An introduction to the wound healing assay using live-cell microscopy. 2014, 8(5), 440-451. DOI: 10.4161/cam.36224. ISSN 1933-6918. Dostupné také z: http://www.tandfonline.com/doi/full/10.4161/cam.36224

[15] MORENO-BUENO, Gema, Héctor PEINADO, Patricia MOLINA, et al. Effects of Concentration and Reaction Time of Trypsin, Pepsin, and Chymotrypsin on the Hydrolysis Efficiency of Porcine Placenta. Nature Protocols. 2009, 4(11), 151-157. DOI: 10.1038/nprot.2009.152. ISSN 1754-2189. Dostupné také z: http://www.nature.com/articles/nprot.2009.152

[16] JUNG, Kyung-Hun, Ye-Chul CHOI, Ji-Yeon CHUN, Sang-Gi MIN a Geun-Pyo HONG. Effects of Concentration and Reaction Time of Trypsin, Pepsin, and Chymotrypsin on the Hydrolysis Efficiency of Porcine Placenta. Korean Journal for Food Science of Animal Resources. 2014, 34(2), 151-157. DOI: 10.5851/kosfa.2014.34.2.151. ISSN 1225-8563.

[17] WEI, Yuanchen, Feng CHEN, Tao ZHANG, Deyong CHEN, Xin JIA, Junbo WANG, Wei GUO a Jian CHEN. A Tubing-Free Microfluidic Wound Healing Assay Enabling the

Quantification of Vascular Smooth Muscle Cell Migration. Scientific Reports. 2015, 5(1), 440-451. DOI: 10.1038/srep14049. ISSN 2045-2322. Dostupné také z: http://www.nature.com/articles/srep14049

[18] NIE, F, M YAMADA, J KOBAYASHI, M YAMATO, A KIKUCHI, T OKANO, Wei GUO a Jian CHEN. On-chip cell migration assay using microfluidic channels. Biomaterials. 2007, 28(27), 4017-4022. DOI: 10.1016/j.biomaterials.2007.05.037. ISSN 01429612. Dostupné také z: https://linkinghub.elsevier.com/retrieve/pii/S0142961207004516

[19] VAN DER MEER, Andries D., Kim VERMEUL, André A. POOT, Jan FEIJEN, István VERMES, T OKANO, Wei GUO a Jian CHEN. A microfluidic wound-healing assay for quantifying endothelial cell migration. American Journal of Physiology-Heart and Circulatory Physiology. 2010, 298(2), H719-H725. DOI: 10.1152/ajpheart.00933.2009. ISSN 0363-6135. Dostupné také z: http://www.physiology.org/doi/10.1152/ajpheart.00933.2009

[20] STICKER, Drago, Sarah LECHNER, Christian JUNGREUTHMAYER, Jürgen ZANGHELLINI, Peter ERTL, T OKANO, Wei GUO a Jian CHEN. Microfluidic Migration and Wound Healing Assay Based on Mechanically Induced Injuries of Defined and Highly Reproducible Areas. Analytical Chemistry. 2017, 89(4), 2326-2333. DOI: 10.1021/acs.analchem.6b03886. ISSN 0003-2700. Dostupné také z: http://pubs.acs.org/doi/10.1021/acs.analchem.6b03886

[21] Thermo Fisher Scientific. Technical Reference Library: The Molecular Probes Handbook: Fluorescence Fundamentals. ThermoFisherScientific [online]. [cit. 2019-05-02]. Dostupné z:https://www.thermofisher.com/us/en/home/references/molecular-probes-the-handbook/introduction-to-fluorescence-techniques.html

[22] Thermo Fisher Scientific. Technical Reference Library: The Molecular Probes Handbook: Molecular Probes School of Fluorescence › Ways to Add Fluorescent Labels. ThermoFisherScientific [online]. [cit. 2019-05-02]. Dostupné z: https://www.thermofisher.com/us/en/home/life-science/cell-analysis/cell-analysis-learning-center/molecular-probes-school-of-fluorescence/imaging-basics/labeling-your-samples/different-ways-to-add-fluorescent-labels.html

[23] Thermo Fisher Scientific [online]. [cit. 2019-05-02]. Dostupné z: https://www.thermofisher.com/order/catalog/product/C3100MP

[24] AUSUBEL, Frederick M., Roger BRENT, Robert E. KINGSTON, David D. MOORE, J.G. SEIDMAN, John A. SMITH a Kevin STRUHL, ed. Current Protocols in Molecular Biology. 2001. DOI: 10.1002/0471142727.mb1410s44.

[25] SANDERSON, M. J., I. SMITH, I. PARKER a M. D. BOOTMAN, SEIDMAN, J.G., John A. SMITH a Kevin STRUHL, ed. Fluorescence Microscopy. Cold Spring Harbor Protocols. 2014, 2001, 2014(10), pdb.top071795-pdb.top071795. DOI: 10.1101/pdb.top071795. ISSN 1559-6095. Dostupné také z: http://www.cshprotocols.org/cgi/doi/10.1101/pdb.top071795

[26] Confocal microscopes: Leica TCS SP8 X. Leica Mikrosystems [online]. [cit. 2019-05-02]. Dostupné z: http://www.leica-microsystems.com/products/confocal microscopes/details/product/leica-tcs-sp8-x/

[27] International Journal of Computer Applications. 2015, 124(12). ISSN 09758887. Dostupné také z: http://www.ijcaonline.org/research/volume124/number12/chaudhari-2015-ijca-905689.pdf

[28] JAN, Jiří. Medical image processing reconstruction and analysis: concepts and methods. Second edition. Boca Raton: CRC Press, 2019. ISBN 978-113-8310-285.

[29] WALEK, Ing. Petr, Ing. Martin LAMOŠ a prof. Ing. Jiří JAN, CSC. Analýza biomedicínských obrazů FEKT VUT v Brně: Počítačová cvičení. Brno: Biomedicínské inženýrství VUT v Brně, 2015. ISBN 978-80-214-4792-9.

[30] MathWorks: Documentation [online]. [cit. 2019-05-02]. Dostupné z: https://www.mathworks.com/help/images/ref/strel.html

[31] Journal of Visualized Experiments. 2018, (138). ISSN 1940-087X. Dostupné také z: https://www.jove.com/video/57691/optimized-scratch-assay-for-vitro-testing-cell-migration-with-an

[32] Ibidi. Labware: Channel Slides μ-Slide III 3in1: Supporting Material: Instructions μ-Slide III 3in1 [online]. [cit. 2019-05-02]. Dostupné z: https://ibidi.com/img/cms/products/labware/channel_slides/S_8031X_Slide_III3in1/IN_8031X_III_3in1.pdf

[33] ThermoFisherScientific: Calcein, AM, cell-permeant dye: [online]. [cit. 2019-05-02]. Dostupné z: https://www.thermofisher.com/order/catalog/product/C3100MP

[34] ThermoFisherScientific: CellTracker™: Manual [online]. [cit. 2019-05-02]. Dostupné z: https://www.thermofisher.com/document-connect/document-

connect.html?id=man0010620&version=a.0&pdfurl=https%3A%2F%2Fassets.thermofisher.com%2FTFS-Assets%2FLSG%2Fmanuals%2Fcelltracker_fluorescent_probes_qrc.pdf&title=UXVpY2sgUmVmOiBDZWxsVHJhY2tlciBGbHVvcmVzY2VudCBQcm9iZXM=

[35] Ibidi. Labware: Channel Slides µ-Slide III 3in1: Supporting Material: Shear Stress and Shear Rates for ibidi µ-Slides - Based on Numerical Calculations [online]. [cit. 2019-05-02]. Dostupné z: https://ibidi.com/img/cms/support/AN/AN11_Shear_stress.pdf

[36] HUANG, Hsiang-Ling, Hsiang-Wei HSING, Tzu-Chia LAI, et al. Trypsin-induced proteome alteration during cell subculture in mammalian cells. Journal of Biomedical Science. 2010, 17(1). DOI: 10.1186/1423-0127-17-36. ISSN 1423-0127. Dostupné také z: http://www.jbiomedsci.com/content/17/1/36

List of used abbreviations

3T3 – **3** day **t**ransfer, inoculum $3{\times}10^5$ cells

HUVEC – **H**uman **U**mbilical **V**ein **E**ndothelial **C**ells

CHO – **C**hinese **H**amster **O**vary

EDTA – **Di**sodium **Et**hylenediaminetetraacetic **A**cid

2D – **Two**-**d**imensional

3D – **Three**-**d**imensional

O_2 – Molecular **O**xygen

CO_2 – **C**arbon di**o**xide

pH – **P**otential of **H**ydrogen

DMEM – **D**ulbecco's **M**odified **E**agle **M**edium

EGM-2 – **E**ndothelial **C**ell **G**rowth **M**edium

PBS – **P**hosphate-**b**uffered **S**aline

FBS – **F**etal **B**ovine **S**erum

EDTA – **Di**sodium **Et**hylenediaminetetraacetic **A**cid

DNA – **D**eoxyribo**n**ucleic **A**cid

PDMS – **P**oly**dim**ethyl**s**iloxane

NIH – National **I**nstitutes of **H**ealth

EBM-2 – **E**ndothelial Cell Growth **B**asal **M**edium

AM – **A**cetoxy**m**ethylester

CMFDA – 5-**c**hloro**m**ethyl**f**luorescein **dia**cetate

HyD – **Hy**brid **D**etector

PMT – **P**hoto-**m**ultiplier **T**ube

LSCM – **L**aser **S**canning **C**onfocal **M**icroscope

SE – **S**tructure **E**lement

WA – **W**ound **A**rea

SD – **S**tandard **D**eviation